Medicine
Immunology and Inflammation

Preeclampsia-specific immune cell network in placenta revealed by Cytometry by time of flight and single-cell RNA-seq

Reviewed Preprint
v1 • September 11, 2024
Not revised

Haiyi Fei, Xiaowen Lu, Zhan Shi, Xiu Liu, Cuiyu Yang, Xiaohong Zhu, Yuhan Lin, Ziqun Jiang, Jianmin Wang, Dong Huang, Liu Liu, Songying Zhang, Lingling Jiang

Assisted Reproduction Unit, Department of Obstetrics and Gynecology, Sir Run Run Shaw Hospital, School of Medicine, Zhejiang University, Hangzhou, 310016, China • Zhejiang Provincial Clinical Research Center for Obstetrics and Gynecology, Hangzhou, 310016, China • Zhejiang Key Laboratory of Precise Protection and Promotion of Fertility, Hangzhou, 310016, China • Department of Obstetrics and Gynecology, Zhejiang Xiaoshan Hospital, 310016, Hangzhou, China

Abstract

Preeclampsia (PE), a major cause of maternal and perinatal mortality with highly heterogeneous causes and symptoms, is usually complicated by gestational diabetes mellitus (GDM). However, a comprehensive understanding of the immune microenvironment in the placenta of PE and the differences between PE and GDM is still lacking. In this study, Cytometry by time of flight (CyTOF) indicated that the frequencies of memory-like Th17 cells ($CD45RA^-CCR7^+IL\text{-}17A^+CD4^+$), memory-like $CD8^+$ T cells ($CD45RA^-CCR7^+CD38^+pAKT^{mid}CD127^{low}$) and pro-inflam Macs ($CD206^-CD163^-CD38^{mid}CD107a^{low}CD86^{mid}HLA\text{-}DR^{mid}CD14^+$) were increased, while the frequencies of $CD69^{hi}Helios^{mid}CD127^{mid}$ γδT cells, anti-inflam Macs ($CD206^+CD163^-CD86^{mid}CD33^+HLA\text{-}DR^+$) and granulocyte myeloid-derived suppressor cells (gMDSCs, $CD11b^+CD15^{hi}HLA\text{-}DR^{low}$) were decreased in the placenta of PE compared with that of NP, but not in that of GDM or GDM&PE. The pro-inflam Macs were positively correlated with memory-like Th17 cells and memory-like $CD8^+$ T cells but negatively correlated with gMDSCs. Single-cell RNA sequencing revealed that transferring the $F480^+CD206^-$ pro-inflam Macs with a $Folr2^+Ccl7^+Ccl8^+C1qa^+C1qb^+C1qc^+$ phenotype from the uterus of PE mice to normal pregnant mice induced the production of memory-like $IL\text{-}17a^+Rora^+Il1r1^+TNF^+Cxcr6^+S100a4^+CD44^+$ Th17 cells via IGF1-IGF1R, which contributed to the development and recurrence of PE. Pro-inflam Macs also induced the production of memory-like $CD8^+$ T cells but inhibited the production of $Ly6g^+S100a8^+S100a9^+Retnlg^+Wfdc21^+$ gMDSCs at the maternal-fetal interface, leading to PE-like symptoms in mice. In conclusion, this study revealed the PE-specific immune cell network, which was regulated by pro-inflam Macs, providing new ideas about the pathogenesis of PE.

eLife assessment

This **valuable** study investigates the immune system's role in pre-eclampsia. The authors map the immune cell landscape of the human placenta and find an increase in macrophages and Th17 cells in patients with pre-eclampsia. Following mouse studies, the authors suggest that the IGF1-IGF1R pathway might play a role in how macrophages influence T cells, potentially driving the pathology of pre-eclampsia. There is **solid** evidence in this study that will be of interest to immunologists and developmental biologists, however, some of the conclusions require additional detail and/or more appropriate statistical tests.

https://doi.org/10.7554/eLife.100002.1.sa3

Introduction

In recent years, low fertility is a global problem (Agbaglo et al., 2022), exacerbated by pregnancy complications. Preeclampsia (PE) is a progressive systemic disease during pregnancy, with pregnancy-induced hypertension, proteinuria, and liver and kidney injury as the main diagnostic indicators (Chappell et al., 2021). With a global prevalence of 7–10%, PE is a major cause of maternal and perinatal mortality and morbidity, especially in low-income and middle-income countries. The only specific treatment is delivery (Chappell et al., 2021). However, due to the variety of symptoms and the heterogeneity of the disease, the pathogenesis of PE is still unclear (Burton et al., 2019; Grotegut, 2016).

PE is often complicated by gestational diabetes mellitus (GDM), which is characterized by insulin resistance and associated with aberrant maternal immune cell adaption (Corrêa-Silva et al., 2018; McElwain et al., 2021; McIntyre et al., 2019). Studies have shown that GDM is an independent risk factor for preeclampsia (Nerenberg et al., 2013; Ostlund et al., 2004; Schneider et al., 2012). However, whether a different pathogenesis underlies between PE and GDM is still unclear.

The fetus is equivalent to a semi-homogenous graft for the mother. Therefore, maternal-fetal immune tolerance plays an important role in the maintenance of pregnancy. Elevated levels of maternal inflammation are now considered to be an important mechanism in the pathogenesis of preeclampsia (Aneman et al., 2020; Deer et al., 2023; Jung et al., 2022), including macrophages (Faas et al., 2014; Yao et al., 2019), granulocytes (Lampé et al., 2015; Lampé et al., 2011; D. Liu et al., 2021), natural killer (NK) cells (Bachmayer et al., 2006; Fukui et al., 2011; Travis et al., 2020), innate B1 cells (Jensen et al., 2012; LaMarca et al., 2011; Zhong et al., 2007) and γδ T cells (Chatterjee et al., 2017). Moreover, adaptive immune response is also critical for the pathogenesis of PE (Deer et al., 2023). In PE, $CD4^+$ T cells prefer to differentiate into pro-inflammatory Th1 and Th17 phenotypes (Eghbal-Fard et al., 2019; Fu et al., 2014; Lang et al., 2021; Lu et al., 2020); Saito et al. (2007) instead of non-inflammatory Th2 and Treg phenotypes (Care et al., 2018; Cornelius et al., 2015a; Saito et al., 2007; Santner-Nanan et al., 2009; Sasaki et al., 2007). However, a comprehensive and in-depth understanding of the maternal-fetal interface of PE is still lacking.

The immune cells crosstalk with each other at the maternal-fetal interface elaborately. The interaction between B2 cells and Th cells depends on CD40 and its ligand CD40L, which helps B2 cells provide AT1-AAs and differentiate into memory B cells (Cornelius et al., 2015b). The

cytokines derived from NK cells can promote the differentiation of Th17 to co-work in recurrent miscarriage (Fu et al., 2013). Nevertheless, studies about the regulation of the immune network at the maternal-fetal interface of PE still need to be completed.

In this study, we combined cytometry by time of flight (CyTOF), single-cell RNA sequencing (scRNA-seq), and rodent experiment to identify the overall immune cell composition and their interactions at the maternal-fetal interface in PE, GDM, and GDM complicated with PE (GDM&PE). This study revealed the PE-specific immune cell network, which was regulated by pro-inflammatory macrophages, providing new ideas about the pathogenesis of PE.

Results

Overall immune cell profile in the placenta of PE, GDM, and GDM&PE

To fully characterize the immune microenvironment at the maternal-fetal interface of PE, we collected full-term placentas of PE and normal pregnancy (NP), and did a CyTOF test (**Table 1**), which panel was shown in **Table 2**. Since PE is usually complicated by GDM, the subjects of GDM and GDM complicated with PE (GDM&PE) were also included. The experimental workflow for CyTOF is shown in the schematic diagram (**Figure 1A**). We found that in addition to the well-known macrophages and T cells, there are also γδ T cells, B cells, NK cells, granulocytes, dendritic cells (DCs), and myeloid-derived suppressor cells (MDSCs). An overall distribution of $CD45^+$ cell subsets in placentas was shown in the t-SNE maps (**Figure 1B**). There were no significant differences in the proportion of these large subpopulations comparing the PE, GDM, GDM&PE group to the NP group (**Figure 1C**). To identify the ten cell subpopulations, CD4, CD8, and γδTCR were used as markers to distinguish $CD4^+$ T cells, $CD8^+$ T cells, and γδ T cells. CD11b is a marker that distinguishes myeloid cells, including macrophages and granulocytes (**Figure 1D**). The ten cell subsets were further annotated by 41 markers in the heatmap (**Figure 1E**, **Table 3**).

Specific altered T cell profile in the placenta of PE

To fully understand the distribution in each cell subset, we first analyzed 15 clusters of $CD4^+$ T cells from the placentas of NP, PE, GDM, and GDM&PE (**Figure 2A**). $CD4^+$ T cell clusters were defined by canonical marker set signatures (**Figure 2-figure supplement 1 A**). The frequencies of memory-like $CD45RA^-CCR7^{mid}CD28^+CD127^+CD4^+$ T cells (cluster 8) were significantly increased in individuals with PE compared with NP controls, while. At the same time, there was no significance in the GDM and GDM&PE groups compared with the NP group (**Figure 2B**, **Table 4**). We analyzed the expression of common intracellular molecules in $CD4^+$ memory-like T cells by sorting $CD45RO^+CCR7^+CD4^+$ T cells from placental samples by flow cytometry. Higher levels of IL-17A and lower levels of Foxp3 were found in memory-like $CD45RO^+CCR7^+CD4^+$ T cells in the placentas of individuals with PE (**Figure 2C**). Consistent with the results of CyTOF, the higher fluorescence intensity of $CD45RO^+CD4^+$ T cells was found in the placentas of individuals with PE (**Figure 2D**). Moreover, lower expression of immune checkpoint molecules including T-cell immunoglobulin mucin-3 (Tim-3) and programmed cell death 1 (PD-1) was found in $CD45RA^-CCR7^+CD4^+$ memory T cells in the PE group, suggesting that these cells have a lower immunosuppressive capacity (Chen et al., 2022; Fanelli et al., 2021; Rasmussen et al., 2022; Wang et al., 2016), though there is no significant difference in the GDM or GDM&PE groups comparing with the NP group (**Figure 2E**). Then, 18 clusters of $CD8^+$ T cells were analyzed (**Figure 2F**). $CD8^+$ T cell clusters annotation was based on the expression of canonical marker signatures (**Figure 2-figure supplement 1 B**). $CD45RA^-CCR7^+CD38^+pAKT^{mid}CD127^{low}$ (cluster 2) memory-like $CD8^+$ T cells were were significantly increased in the PE group (**Figure 2G**, **Table 4**). Cluster 2 expressed lower expression of PD-1 and TIGIT, suggesting the activation of

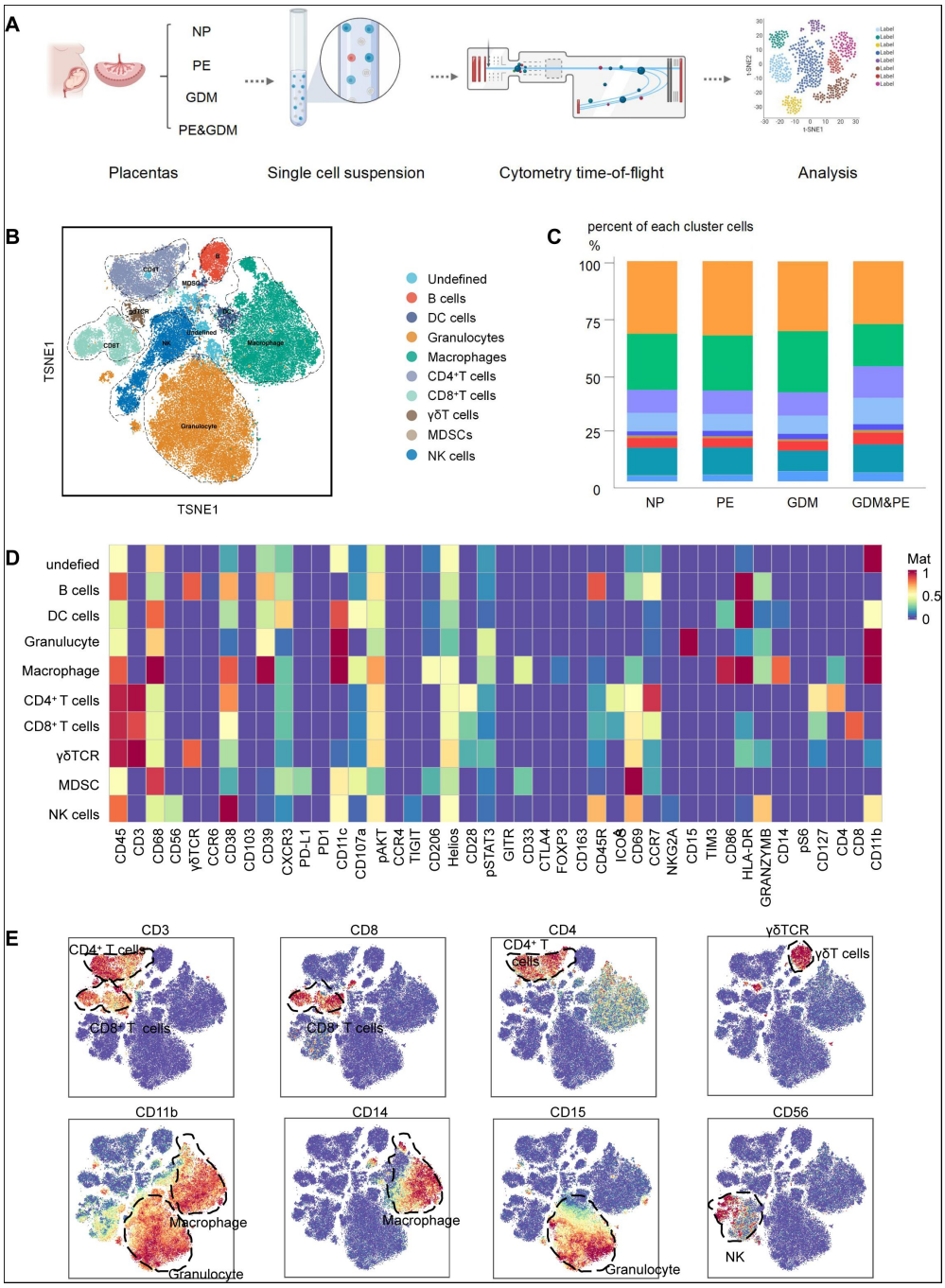

Figure 1

Identification and characterization of placental immune cells using CyTOF

(A) Schematic of the experimental workflow in CyTOF experiment. The placentas were obtained from individuals with normal pregnancy (NP, n=9), preeclampsia (PE, n=8), gestational diabetes mellitus (GDM, n=8) or GDM&PE (n=7).
(B) t-SNE maps showing 7×10^5 $CD45^+$ cells from the placenta overlaid with color-coded clusters and the distributions of B cells, $CD4^+$ T cells, $CD8^+$ T cells, DC, γδT cells, monocytes, granulocytes, MDSC, and NK cells.
(C) Percentages of each cell type of $CD45^+$ cells in placentas.
(D) t-SNE maps showing the expression of CD3, CD8, CD4, γδTCR, CD14, CD15, CD56.
(E) Heatmap showing the expression levels of markers in $CD45^+$ cell subsets.
Data were compared between NP and PE, NP and GDM, NP and GDM&PE using the Shapiro-wilk test and represented as mean±SEM (*P < 0.05, ** P < 0.01, *** P < 0.001; NS, not significant).

Parameters	NP (n=9)	PE (n=8)	GDM (n=8)	GDM&PE (n=7)	p Value
Age (years)	31.33 ± 2.108	31.75 ± 4.206	35.25 ±3.419	32.43 ± 2.321	0.1008
BMI (kg/m^2)	27.35 ± 1.740	30.84 ±2.888	29.56 ± 2.689	30.16 ± 2.280	0.0518
Gestational age (weeks)	38.89 ± 0.558	37.39 ± 1.253	38.73 ± 0.419	36.22 ± 1.372	<0.001
Number of living children	0.4444 ± 0.497	0.500 ± 0.500	1.125 ± 0.331	0.429 ± 0.495	0.0236
Previous abortions	0.7778 ± 1.030	1.000 ± 0.866	1.000 ± 1.000	1.714 ± 2.050	0.5848
Mean Systolic Blood Pressure	109.7 ± 5.400	151 ± 7.225	106.9 ± 2.848	150.7 ± 9.161	<0.0001

Table 1

Details of the individuals included in the CyTOF

Target	Metal tag
CD45	HI30
CD3	UCHT1
CD68	Y1/82A
CD56	NCAM16.2
gd TCR	5A6.E9
CD19	HIB19
CCR6	G034E3
CD38	HIT2
CD103	B-Ly7
CD39	A1
CXCR3	G025H7
PD-L1	29E.2A3
PD-1	EH12.2H7
CD11C	BU15
CD107a	H4A3
pAKT	D9E
CCR4	L291H4
TIGIT	A15153G
CD206	15-2
Helios	22F6
CD28	CD28.2
pSTAT3	4/p-Stat3
GITR	110416
CD33	WM53
CTLA-4	BN13
FOXP3	PCH101
CD163	GHI/61
CD45RA	HI100
ICOS	C398.4A
CD69	FN50
CCR7	G043H7
NKG2A	131411
CD15	W6D3
TIM-3	F38-2E2
CD86	Fun-1
HLA-DR	L243
Granzyme B	QA16A02
CD14	M5E2
pS6	A17020B
CD127	A019D5
CD4	RPA-T4
CD8	RPA-T8
CD11b	M1/70

Table 2

CyTOF antibody panel used for analyzing placentas from individuals with normal pregnancy (NP), preeclampsia (PE), gestational diabetes mellitus (GDM) and GDM complicated with PE (GDM&PE)

	B cells	CD4$^+$ T	CD8$^+$ T	gdTCR	NK cells	Macrophage	Granulocyte	MDSC	Dendritic cells
CD45	++	++	++	++	++	++	++	++	++
CD3	-	++	++	-	-	-	-	-	-
CD68	+	+	+	+	+	++	+	++	++
CD56	-	-	-	-	+	-	-	-	-
gd TCR	++	-	-	++	-	-	-	-	-
CD19	++	-	-	++	-	-	-	-	-
CCR6	+	-	-	-	-	-	-	-	-
CD38	++	++	+	+	++	++	-	-	+
CD103	-	-	-	-	-	-	-	-	-
CD39	++	-	-	-	+	++	+	+	+
CXCR3	+	+	+	+	+	+	-	+	++
PD-L1	-	-	-	-	-	-	-	+	-
PD-1	-	-	-	-	-	-	-	-	-
CD11C	+	-	-	-	+	++	++	+	++
CD107a	+	-	-	-	-	+	-	+	+
pAKT	+	+	+	+	+	++	+	+	+
CCR4	-	-	-	-	-	-	-	-	-
TIGIT	-	-	-	-	-	-	-	-	-
CD206	-	-	-	-	-	+	-	+	-
Helios	+	+	+	+	+	+	+	+	+
CD28	-	+	+	+	-	-	-	-	-
pSTAT3	+	+	-	+	-	+	+	-	-
GITR	-	-	-	-	-	-	-	-	-
CD33	-	-	-	-	-	+	-	+	-
CTLA-4	-	-	-	-	-	-	-	-	-
FOXP3	-	-	-	-	-	-	-	-	-
CD163	-	-	-	-	-	-	-	-	-
CD45RA	++	+	+	+	++	-	-	-	-
ICOS	-	+	+	-	-	-	-	-	-
CD69	+	+	+	+	++	+	-	++	-
CCR7	+	++	+	+	-	-	-	+	-
NKG2A	-	-	-	-	-	-	-	-	-
CD15	-	-	-	-	-	-	++	-	-
TIM-3	-	-	-	-	-	-	-	-	-
CD86	-	-	-	-	-	++	-	-	+
HLA-DR	++	-	+	+	-	++	+	-	++
Granzyme	+	-	-	+	++	+	+	-	-
CD14	-	-	-	-	-	++	-	-	-
pS6	-	-	-	-	-	-	-	-	-
CD127	-	++	+	-	-	-	-	-	-
CD4	-	++	-	-	-	-	-	-	-
CD8	-	-	++	-	-	-	-	-	-
CD11b	-	-	-	+	+	++	++	-	+

Table 3

Expression levels of markers identified in each immune subset in the placentas

cytotoxicity of these cells (**Figure 2H**) (Morita et al., 2020). Then, 22 clusters of γδT cells were analyzed and annotated (**Figure 2I**, **Figure 2-figure supplement 1 C**). Cluster 15, which expressed lower expression of Tim3, was significantly decreased in the PE group (**Figure 2J**, **2K**). However, regardless of $CD4^+$ T cells or $CD8^+$ T cells, there is no significant change in the memory-like clusters in the GDM or GDM&PE group compared to the NP group.

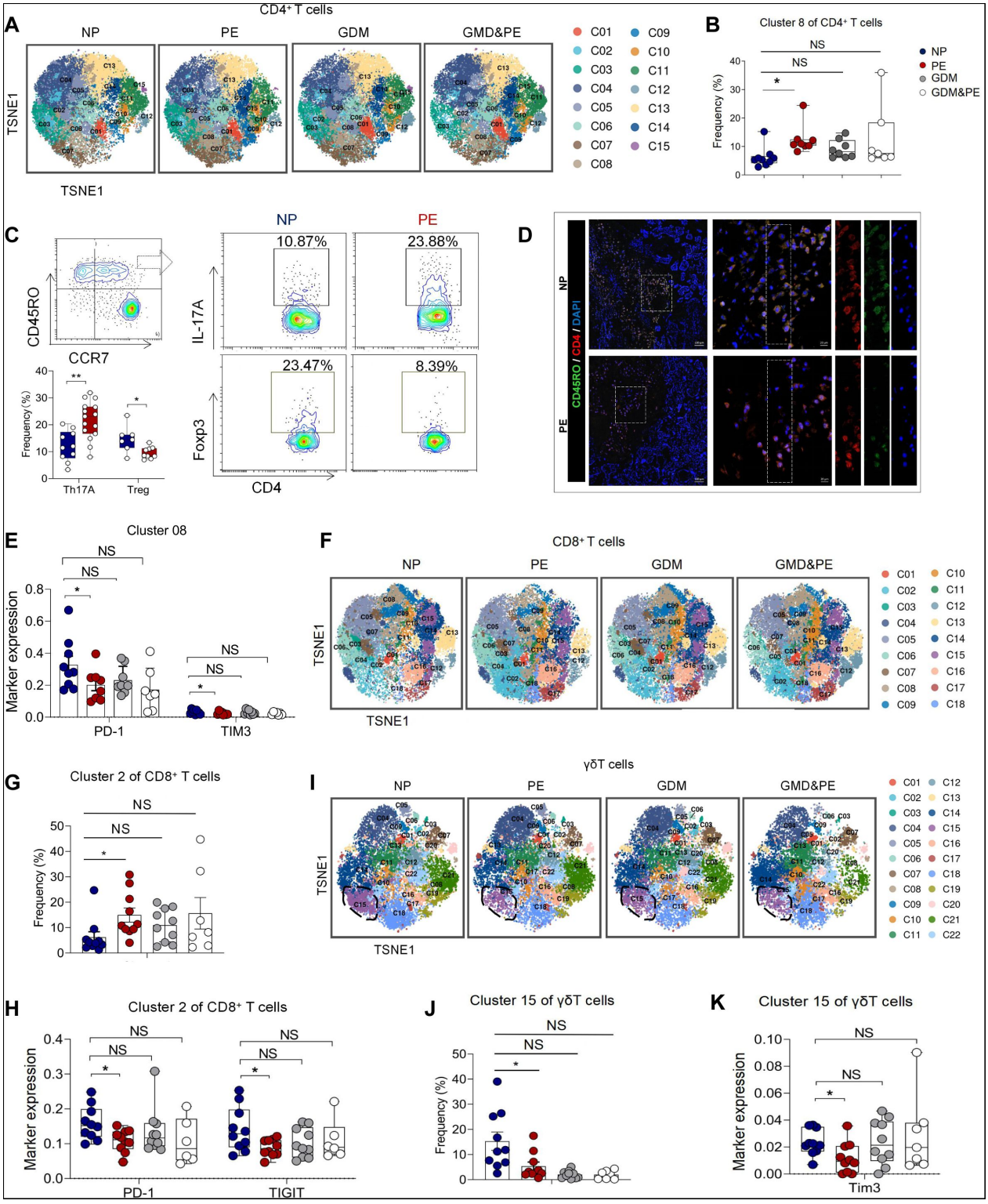
A
CD4⁺ T cells
NP
PE
GDM
GMD&PE
TSNE1
TSNE1
B
Cluster 8 of CD4⁺ T cells
NS
NS
*
Frequency (%)
NP
PE
GDM
GDM&PE
C
NP
PE
10.87%
23.88%
CD45RO
CCR7
IL-17A
23.47%
8.39%
Foxp3
CD4
**
*
Frequency (%)
Th17A
Treg
D
NP
PE
CD45RO / CD4 / DAPI
E
Cluster 08
NS
NS
*
NS
NS
*
Marker expression
PD-1
TIM3
F
CD8⁺ T cells
NP
PE
GDM
GMD&PE
TSNE1
TSNE1
G
Cluster 2 of CD8⁺ T cells
NS
NS
*
Frequency (%)
I
γδT cells
NP
PE
GDM
GMD&PE
TSNE1
TSNE1
H
Cluster 2 of CD8⁺ T cells
NS
NS
*
NS
NS
*
Marker expression
PD-1
TIGIT
J
Cluster 15 of γδT cells
NS
NS
*
Frequency (%)
K
Cluster 15 of γδT cells
NS
NS
*
Marker expression
Tim3

Figure 2

Specific altered T cell profile in the placentas of individuals with PE

(A) Distribution of the $CD4^+$ T cells analyzed using t-SNE.

(B) Scatter dot plots showing the frequencies of cluster 8 of $CD4^+$ T cells in the placentas of individuals with NP, PE, GDM and GDM&PE.

(C) Expression of IL-17A and Foxp3 in $CD45RO^+CCR7^+CD4^+$ T cells in placentas of individuals with NP and PE using flow cytometry. (IL-17A: n=10 in NP group, n=15 in PE group; Foxp3: n=7 in NP group, n=9 in PE group).

(D) Immunofluorescence co-staining of CD4 (red), CD45RO (green) and DAPI (blue) in frozen placental sections. The right panels show the enlargement of the dotted box in the left panel. Scale bar, 20 μm.

(E) Scatter dot plots showing significantly altered markers of in cluster 8 of $CD4^+$ T cells.

(F) Distribution of the $CD8^+$ T cells analyzed using t-SNE.

(G) Scatter dot plots showing the frequencies of cluster 2 of $CD8^+$ T cells in the placentas of individuals with NP, PE, GDM and GDM&PE.

(H) Scatter dot plots showing significantly altered markers in cluster 2 of $CD8^+$ T cells.

(I) Distribution of the γδT cells analyzed using t-SNE.

(J) Scatter dot plots showing the frequencies of cluster 15 of γδT cells in the placentas of individuals with NP, PE, GDM and GDM&PE.

(K) Scatter dot plots showing significantly altered markers in cluster 15 of γδT cells.

Data were compared between NP and PE, NP and GDM, NP and GDM&PE using the Shapiro-wilk test and represented as mean±SEM (*P < 0.05, ** P < 0.01, *** P < 0.001; NS, not significant).

In conclusion, significant changes in placental T cell profile were found in the placentas of PE but not in those of GDM or GDM&PE, suggesting that abnormal activation of T cells in the placenta is associated with the pathogenesis of PE.

Abnormal polarization of macrophages was correlated with specific immune cell subsets in individuals with PE

Except for T cells, we also analyzed 29 clusters of $CD45^+CD3^-CD11b^+$ cells from placentas of NP, PE, GDM, and GDM&PE, including 9 clusters of macrophages, 11 clusters of granulocytes, and 5 clusters of NK/NK-like cells (**Figure 3A**). The clusters of $CD45^+CD3^-CD11b^+$ cells were defined by canonical marker set signatures (**Figure 3 B**). Moreover, significantly decreased frequencies of $CD11b^+CD15^{hi}HLA\text{-}DR^{low}$ granulocytes (cluster 12), which are identified as granulocyte myeloid-derived suppressor cells (gMDSCs), were found in the PE group (**Figure 3C**, **Table 4**). In addition, the frequency of anti-inflammatory macrophages (anti-inflam Macs) ($CD206^+CD163^-CD86^{mid}CD33^+HLA\text{-}DR^+$, cluster 25) was also significantly decreased, whereas the frequency of pro-inflammatory macrophages (pro-inflam Macs) ($CD206^-CD163^-CD38^{mid}CD107a^{low}CD86^{mid}$HLA-

	memory-like $CD4^+$ T cells Cluster 08 of $CD4^+$ T cells	memory-like $CD8^+$ T cells Cluster 02 of $CD8^+$ T cells	gMDSCs Cluster 12 of $CD3^-CD11b^+$ cells	pro-inflammatory macrophages Cluster 23 of $CD3^-CD11b^+$ cells	anti-inflammatory macrophages Cluster 25 of $CD3^-CD11b^+$ cells
CD45	++	++	++	++	++
CD3	++	++	-	-	-
CD68	-	-	+	++	++
CD56	-	-	-	-	-
gd TCR	-	-	-	-	-
CD19	-	-	-	-	-
CCR6	-	-	-	-	-
CD38	++	++	-	+	+
CD103	-	-	-	+	+
CD39	+	-	+	-	-
CXCR3	+	+	-	-	-
PD-L1	-	-	-	-	-
PD-1	-	-	-	-	-
CD11C	-	-	++	++	++
CD107a	-	-	-	+	+
pAKT	+	+	-	-	-
CCR4	-	-	-	-	-
TIGIT	-	-	-	-	-
CD206	-	-	+	-	+
Helios	+	+	-	-	-
CD28	+	+	-	-	-
pSTAT3	-	-	-	-	-
GITR	-	-	-	-	-
CD33	-	-	-	-	+
CTLA-4	-	-	-	-	-
FOXP3	-	-	-	-	-
CD163	-	-	-	-	-
CD45RA	-	-	-	-	-
ICOS	+	+	-	-	-
CD69	+	-	-	-	-
CCR7	++	++	-	-	-
NKG2A	-	-	-	-	-
CD15	-	-	++	-	-
TIM-3	-	-	-	-	-
CD86	-	-	-	+	+
HLA-DR	-	-	+	+	++
Granzyme B	-	-	+	-	-
CD14	-	-	-	+	+
pS6	-	-	-	-	-
CD127	+	-	-	-	-
CD4	++	-	-	-	-
CD8	-	++	-	-	-
CD11b	-	-	++	++	++

Table 4

The marker profile of PE-specific immune subsets

DR^{low} granulocytes (cluster 12), which are identified as granulocyte myeloid-derived suppressor cells (gMDSCs), were found in the PE group (**Figure 3C**, **Table 4**). In addition, the frequency of anti-inflammatory macrophages (anti-inflam Macs) ($CD206^{+}CD163^{-}CD86^{mid}CD33^{+}HLA\text{-}DR^{+}$, cluster 25) was also significantly decreased, whereas the frequency of pro-inflammatory macrophages (pro-inflam Macs) ($CD206^{-}CD163^{-}CD38^{mid}CD107a^{low}CD86^{mid}HLA\text{-}DR^{mid}CD14^{+}$, cluster 23) was significantly increased in the PE group (**Figure 3C**, **Table 4**). However, the frequencies of macrophages and gMDSCs were unchanged significantly in the GDM or GDM&PE groups.

Pearson correlation analysis indicated positive correlations between pro-inflam Macs (cluster 23 in $CD11b^{+}$ cells) and $CD4^{+}$ memory-like T cells (cluster 8 of $CD4^{+}$ T cells), as well as $CD8^{+}$ memory-like T cells (cluster 2 in $CD8^{+}$ T cells). $CD206^{-}$ pro-inflam Macs were negatively correlated with gMDSCs (cluster 12 in $CD11b^{+}$ cells), but were not statistically significant. Conversely, $CD206^{+}$ anti-inflam Macs (cluster 25 in $CD11b^{+}$ cells) were positively correlated with gMDSCs and negatively correlated with $CD8^{+}$ memory-like T cells (**Figure 3D**, **3E**).

These results suggested that abnormally polarized CD206⁻pro-inflam Macs are positively correlated with memory-like $CD4^{+}$ and $CD8^{+}$ T cells in the placentas of individuals with PE and negatively correlated with gMDSCs.

$F480^{+}CD206^{-}$ pro-inflam Macs induced immune imbalance at the maternal-fetal interface and PE-like symptoms

Though increased pro-inflam Macs have been reported in the placenta from individuals with PE (Faas et al., 2014), few studies have reported the interaction between macrophages and other immune cells in the placenta. $CD45^{+}F4/80^{+}CD206^{-}$ pro-inflam Macs or $CD45^{+}F4/80^{+}CD206^{+}$ anti-inflam Macs were isolated from the uterus and placentas of mice with RUPP and injected into normal pregnant mice (**Figure 4A**). RNA-seq was used to analyse the difference between $CD45^{+}F4/80^{+}CD206^{-}$ pro-inflam Macs and $CD45^{+}F4/80^{+}CD206^{+}$ anti-inflam Macs. Significant differences were found between the two groups of macrophages (**Figure 4B**). We found that the expression of 2123 genes was increased, and 2699 genes decreased significantly in the pro-inflam Macs compared to the anti-inflam Macs (**Figure 4C**). The expression levels of genes associated with inflammatory response (Ccl7, Ccl8, Ccl2, IL6) (He et al., 2019; Wu et al., 2023), complement system activation (C1qa, C1qb) (Chen et al., 2021), and lipid metabolism (Pltp, Apoe) (Desrumaux et al., 2016) were significantly increased in the pro-inflam Macs; whereas the expression levels of genes associated with the regulation of angiogenesis and vascular endothelial growth factor production (VEGFα, Macro) and tissue development (TGF-β1, Thbs1, Fn1, Slpi) (Jin et al., 2023; Nugteren et al., 2021; Li et al., 2022) were significantly decreased (**Figure 4C**, **4D**). Moreover, Gene Set Enrichment Analysis (GSEA) was performed to further explore the most significantly enriched functional terms between the two groups of macrophages. We found that NF-κB signaling and interspecies interaction between organisms were enriched in the pro-inflam Macs, while tissue development and epithelial cell morphogenesis were enriched in the anti-inflam Macs (**Figure 4E**).

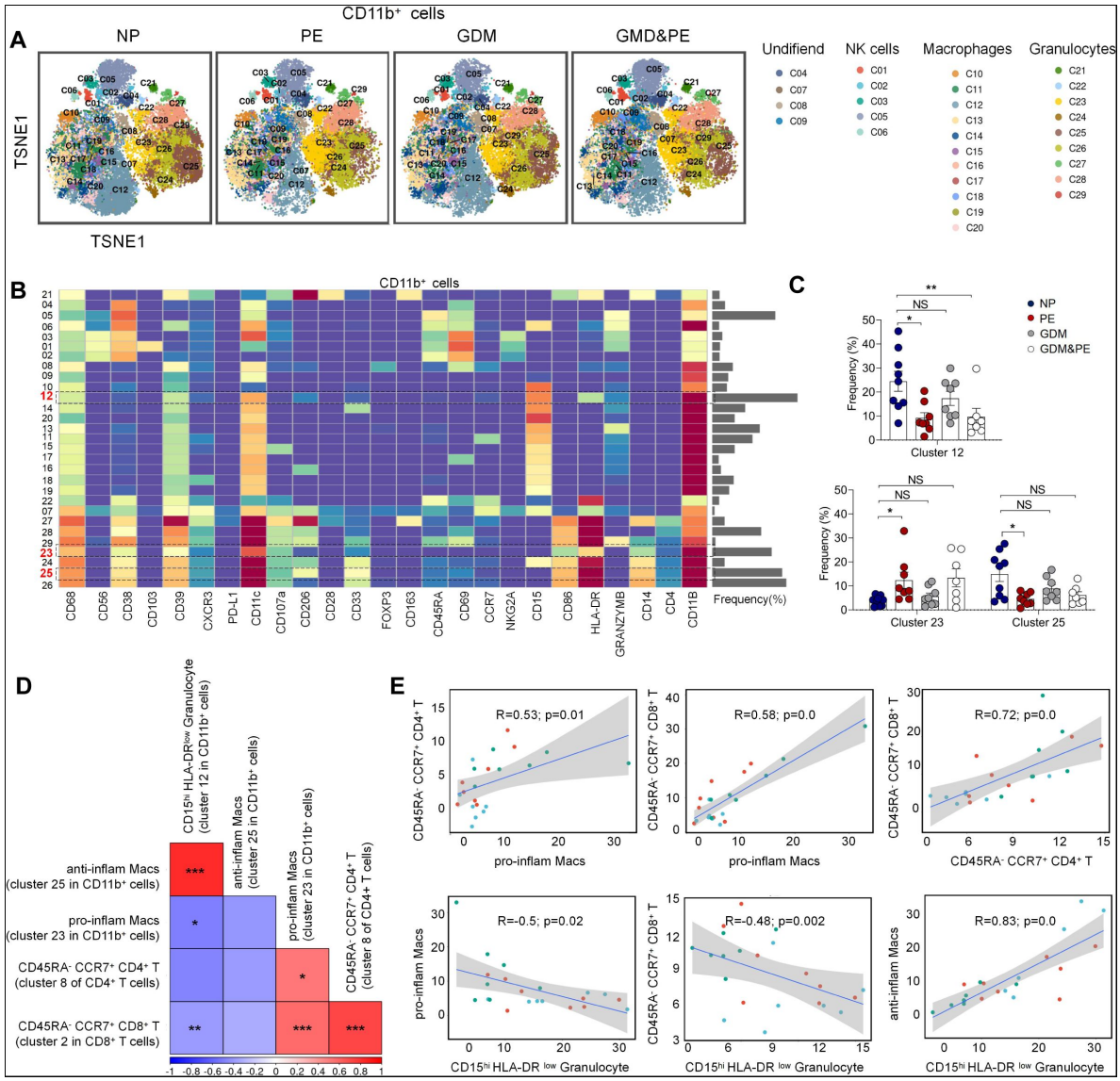

Figure 3

Identification of the placental CD11b$^+$ cell subsets and the Interaction between placental immune cells.

(A) Distribution of the CD11b$^+$ immune cells analyzed using t-SNE.
(B) Heatmap showing the expression levels of markers in the CD11b$^+$ cells.
(C) Scatter dot plots showing the frequencies of cluster 12, cluster 23, and cluster 25 of CD11b$^+$ cells in the placentas.
(D) Interaction between placental immune cells showed in heatmap.
(E) Scatter plots of Pearson's correlation analysis between placental immune cells.
Data were compared between NP and PE, NP and GDM, NP and GDM&PE using the Shapiro-wilk test and represented as mean±SEM (*P < 0.05, ** P < 0.01, *** P < 0.001).

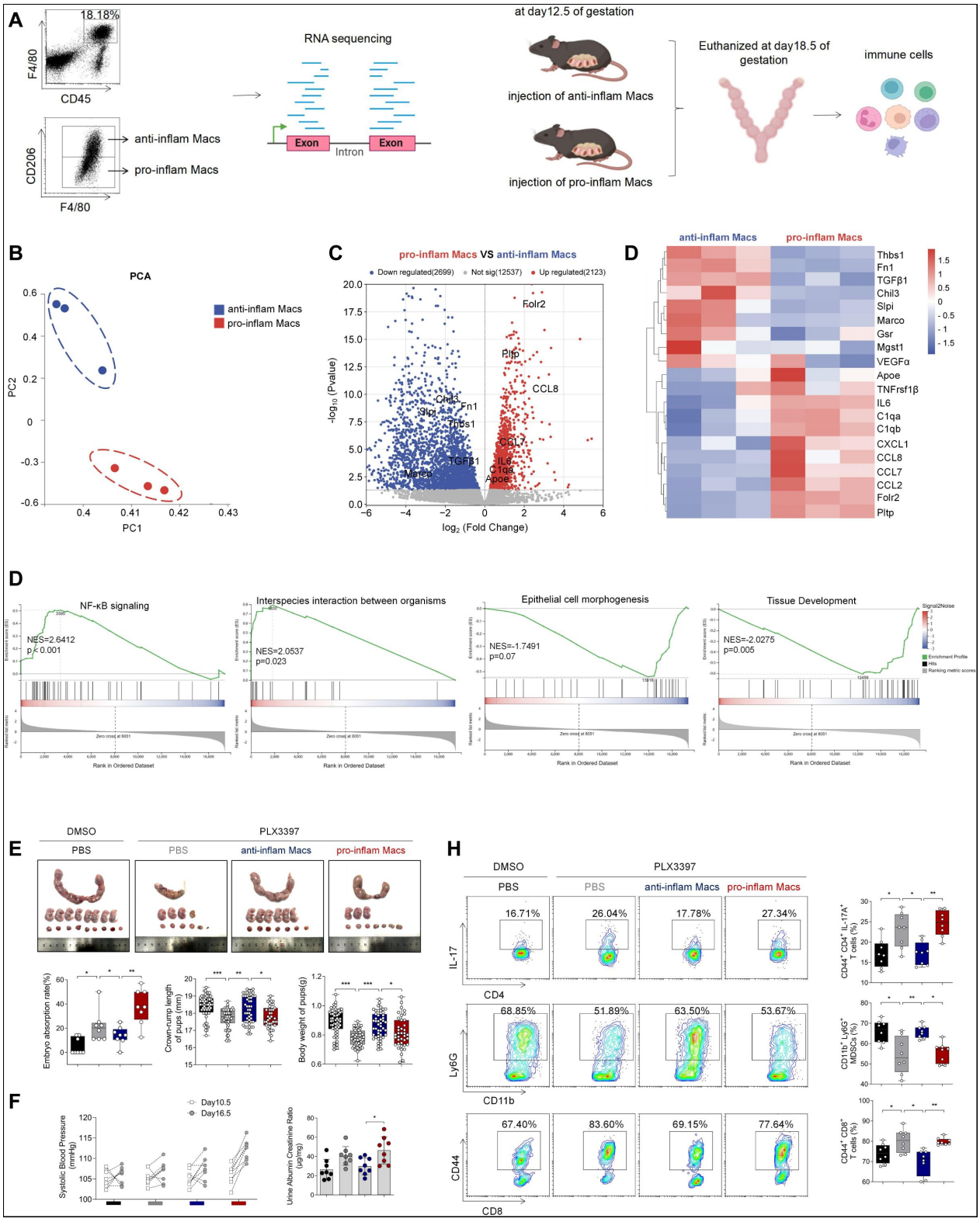
A
18.18%
F4/80
CD45
CD206
F4/80
anti-inflam Macs
pro-inflam Macs
RNA sequencing
Exon
Intron
Exon
at day12.5 of gestation
injection of anti-inflam Macs
injection of pro-inflam Macs
Euthanized at day18.5 of gestation
immune cells
B
PCA
anti-inflam Macs
pro-inflam Macs
PC2
PC1
C
pro-inflam Macs VS anti-inflam Macs
Down regulated(2699)
Not sig(12537)
Up regulated(2123)
-log10 (Pvalue)
log2 (Fold Change)
Folr2
Pltp
CCL8
Chil3
Slpi
Fn1
Thbs1
CCL7
TGFβ1
IL6
C1qa
Marco
Apoe
D
anti-inflam Macs
pro-inflam Macs
Thbs1
Fn1
TGFβ1
Chil3
Slpi
Marco
Gsr
Mgst1
VEGFα
Apoe
TNFrsf1β
IL6
C1qa
C1qb
CXCL1
CCL8
CCL7
CCL2
Folr2
Pltp
D
NF-κB signaling
NES=2.6412
p < 0.001
Interspecies interaction between organisms
NES=2.0537
p=0.023
Epithelial cell morphogenesis
NES=-1.7491
p=0.07
Tissue Development
NES=-2.0275
p=0.005
Rank in Ordered Dataset
E
DMSO
PLX3397
PBS
PBS
anti-inflam Macs
pro-inflam Macs
Embryo absorption rate(%)
Crown-rump length of pups (mm)
Body weight of pups(g)
F
Day10.5
Day16.5
Systolic Blood Pressure (mmHg)
Urine Albumin Creatinine Ratio (μg/mg)
H
DMSO
PLX3397
PBS
PBS
anti-inflam Macs
pro-inflam Macs
16.71%
26.04%
17.78%
27.34%
IL-17
CD4
68.85%
51.89%
63.50%
53.67%
Ly6G
CD11b
67.40%
83.60%
69.15%
77.64%
CD44
CD8
CD44+ CD4+ IL-17A+ T cells (%)
CD11b+ Ly6G+ MDSCs (%)
CD44+ CD8+ T cells (%)

Figure 4

The immune imbalance at the maternal-fetal interface induced by F480^{+}CD206^{-} pro-inflam Macs.

(A) Schematic of the mice model adoptively transferred CD45^{+}F4/80^{+}CD206^{-} pro-inflam Macs or CD45^{+}F4/80^{+}CD206^{+} anti-inflam Macs.

(B) Principal component analysis (PCA) reflected the differences between the two groups of macrophages (n=3).

(C) The volcano map shows a comparison of the content and P value of gene expression between pro-inflam Macs and anti-inflam Macs. Differential expression genes were screened out when P < 0.05. Red dots indicate genes with increased expression in pro-inflam Macs. Blue dots indicate genes with decreased expression.

(D) The volcano map shows differential expression genes between pro-inflam Macs and anti-inflam Macs.

(E) Representative pathways enriched in the identified genes as determined by GSEA (p value<0.05).

(F) Embryo abortion rate of the pregnant mice, body weight and crown-rump length of pups measured on day 18.5 of gestation. Black represents mice treated with DMSO (n=8); gray represents mice treated with PLX3397 (n=8); blue represents mice injected with CD45^{+}F4/80^{+}CD206^{+} anti-inflammatory macrophages (n=8); red represents mice injected with CD45^{+}F4/80^{+}CD206^{-} pro-inflammatory macrophages (n=8).

(G) SBP and UACR of pregnant mice in the four groups.

(H) Frequencies of CD44^{+}CD4^{+}IL-17A^{+} cells, CD44^{+}CD8^{+} T cells and CD11b^{+}Ly6G^{+} granulocytes analyzed by flow cytometry.

To further investigate the effect of the pro-inflam Macs polarization in immune imbalance at the maternal-fetal interface, PLX3397, the inhibitor of CSF1R, which is needed for macrophage development, was used to deplete the macrophages of pregnant mice (X. Chen et al., 2023; J. Chen et al., 2022). As expected, an increased embryo resorption rate, decreased fetal top-rump length and fetal weight were found in mice injected with pro-inflam Macs (**Figure 4F**). Increased SBP and UACR were also found in mice injected with pro-inflam Macs (**Figure 4G**). Moreover, it is shown that CD44^{+} memory-like Th17 cells and memory-like CD8^{+} T cells increased while CD11b^{+}Ly6G^{+} gMDSCs decreased in mice injected pro-inflam Macs compared with mice injected anti-inflam Macs, which validated our findings in CyTOF (**Figure 4H**). Clodronate liposomes were also used to deplete the macrophages of pregnant mice (X. Liu et al., 2022) before pro-inflam Macs or anti-inflam Macs were injected into the mice. The same experimental results were obtained (**Figure 4-figure supplement 1**). In conclusion, the F480^{+}CD206^{-} pro-inflam Macs induced immune imbalance at the maternal-fetal interface and PE-like symptoms.

Pro-inflam Macs and anti-inflam Macs subsets are functionally heterogeneous

To further explore the role that macrophages play in the immune imbalance at the maternal-fetal interface in PE, scRNA-seq was performed to analyze the uterine CD45^{+} immune cells from mice that were transferred with pro-inflam Macs or anti-inflam Macs from the the uterus and placentas of PE mice. An unsupervised cluster detection algorithm (SEURAT) was applied and eight types of immune cells were detected by mostly distinguishable cell type-specific genes, including macrophages, monocytes, granulocytes, T/NK cells, B cells, plasma, mast cells, and basophils (**Figure 5A**, **5B**).

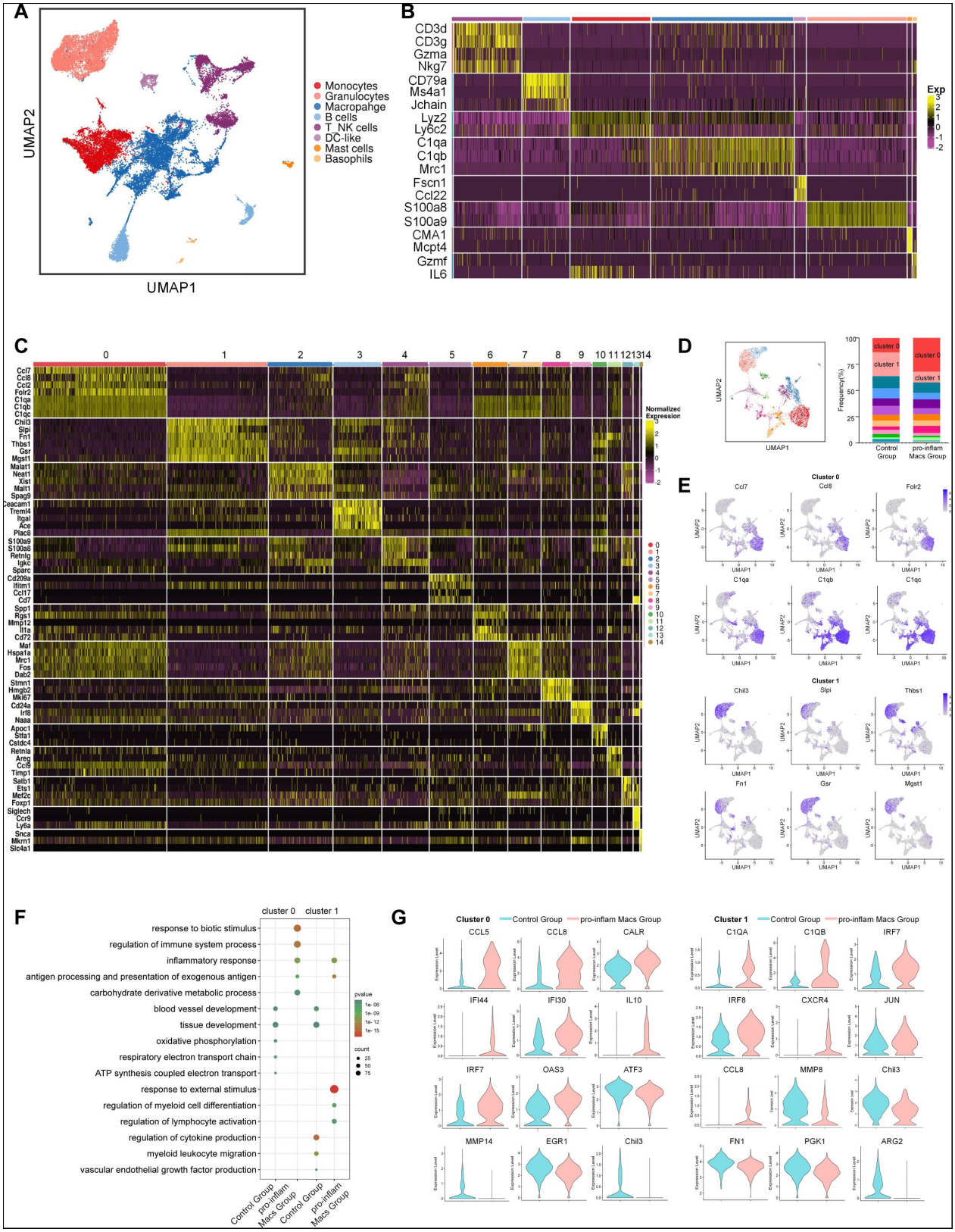
A
UMAP2
UMAP1
Monocytes
Granulocytes
Macropahge
B cells
T_NK cells
DC-like
Mast cells
Basophils
B
CD3d
CD3g
Gzma
Nkg7
CD79a
Ms4a1
Jchain
Lyz2
Ly6c2
C1qa
C1qb
Mrc1
Fscn1
Ccl22
S100a8
S100a9
CMA1
Mcpt4
Gzmf
IL6
Exp
C
Normalized Expression
D
UMAP2
UMAP1
Frequency(%)
cluster 0
cluster 1
Control Group
pro-inflam Macs Group
E
Cluster 0
Ccl7
Ccl8
Folr2
C1qa
C1qb
C1qc
Cluster 1
Chil3
Slpi
Thbs1
Fn1
Gsr
Mgst1
F
cluster 0
cluster 1
response to biotic stimulus
regulation of immune system process
inflammatory response
antigen processing and presentation of exogenous antigen
carbohydrate derivative metabolic process
blood vessel development
tissue development
oxidative phosphorylation
respiratory electron transport chain
ATP synthesis coupled electron transport
response to external stimulus
regulation of myeloid cell differentiation
regulation of lymphocyte activation
regulation of cytokine production
myeloid leukocyte migration
vascular endothelial growth factor production
pvalue
count
Control Group
pro-inflam Macs Group
G
Cluster 0
Control Group
pro-inflam Macs Group
CCL5
CCL8
CALR
IFI44
IFI30
IL10
IRF7
OAS3
ATF3
MMP14
EGR1
Chil3
Cluster 1
C1QA
C1QB
IRF7
IRF8
CXCR4
JUN
CCL8
MMP8
Chil3
FN1
PGK1
ARG2

Figure 5

Identification of the macrophage subsets in mice injected pro-inflam Macs and anti-inflam Macs use sc RNA-seq.

(A) UMAP maps showing the 8 types of mouse immune cells at the maternal-fetal interface.

(B) Heatmap showing clustering analysis for markers distinguished different type of immune cells.

(C) Heatmap showing clustering analysis for markers distinguished different clusters of macrophages.

(D) UMAP maps showing the 15 clusters of mouse macrophages was listed in the left panel. Bar graph showing the frequencies of clusters of macrophages in the two groups of mice was listed in the right panel.

(E) UMAP maps showing the distribution of specific markers of cluster 0 and cluster 1.

(F) Dot plot depicting GO enrichment terms that were significantly enriched in the differentially expressed genes in cluster 0 and cluster 1 from the pro-inflam Macs group and the control group.

(G) Violin plot of specific differential gene expression in cluster 0 and cluster 1 between the pro-inflam Macs group and the control group.

Macrophages were further identified into 15 clusters defined by marker set signatures. Single-cell differential expression analysis (SCDE) was performed for each population and characteristic gene expression patterns were detected for cluster 0-cluster 14 to characterize the phenotypes of these subsets in detail (**Figure 5C**). We found that the frequency of cluster 0 was significantly increased in mice injected with pro-inflam Macs, while the frequency of cluster 1 was significantly decreased (**Figure 5D**). We also found that cluster 0 highly expresses genes associated with foetal and tissue resident (Folr2) (Nalio et al., 2022; Thomas et al., 2021), complement system activation (C1qa, C1qb, C1qc) (Chen et al., 2021), and inflammatory response (Ccl7, Ccl8) (He et al., 2019; Wu et al., 2023); while cluster 1 highly expresses genes associated with tissue repair (Chil3, Slpi, Fn1) (Jin et al., 2023; Nugteren et al., 2021; Li et al., 2022), blood vessel morphogenesis (Thbs1) (Che et al., 2021) and preventing oxidative stress (Gsr, Mgst1) (Coppo et al., 2022) (**Figure 5E**). Changes in gene expression patterns of cluster 0 (pro-inflam Macs) and cluster 1 (anti-inflam Macs) were analyzed in mice injeced the pro-inflam Macs or anti-inflam Macs. We found that in the pro-inflam Macs group, enriched GO terms in cluster 0 and cluster1 including ‘antigen processing and presentation of exogenous antigen’ and ‘inflammatory response’, in which high expression of genes such as CCL5, CCL8, CALR, IRF7, IL10, IFI44, IFI30, OAS3, etc. could be observed (**Figure 5F**, **5G**). The control group showed elevated expression of MMP14, Chil3, EGR1, ATF3 and VASP; and these genes were enriched in ‘vascular endothelial growth factor production’ and ‘tissue development’ (**Figure 5F**, **5G**). These results were consistent with the results of the transcriptome RNA sequencing results of macrophages.

These data suggested that the $CD45^{+}F480^{+}CD206^{-}$ pro-inflam Macs with a $Folr2^{+}Ccl7^{+}Ccl8^{+}C1qa^{+}C1qb^{+}C1qc^{+}$ phenotype play an improtant role in the development of PE.

Pro-inflam Macs induced the memory-like Th17 cells, which was associatied with the development and recurrence of PE

We also analyzed the scRNA-seq data of uterine T/NK cells from mice that were injected with or without pro-inflam Macs. T/NK cells were further identified into 12 clusters defined by marker set signatures (**Figure 6A**, **6B**). We found that the frequency of cluster 0 was increased in mice

injected with pro-inflam Macs, while the frequency of cluster 1 and cluster 2 were significantly decreased (**Figure 6A**). In addition to genes associated with Th17 cells (IL-17a, IL17f, Rora, Il1r1, TNF) (Wu et al., 2019; Leite et al., 2023), cluster 0 also exhibits high expression of genes associated with memory phenotype (Cxcr6, S100a4, CD44) (Schroeder et al., 2023; Bieberich et al., 2021), suggesting that cluster 0 was the memory-like Th17 cells (**Figure 6A**, **6C**). Cluster 1 exhibits high expression of genes associated with immunoregulation (Lef1, Tcf7, Ccr7) (Qiu et al., 2022; Sekine et al., 2020); Cluster 2 exhibits high expression of genes associated with immunosuppression (Gata3, GITR, CD28), suggesting that cluster 1 and 2 were T cells with immunosuppressive function (Esensten et al., 2016; Pai et al., 2023) (**Figure 6A**, **6C**).

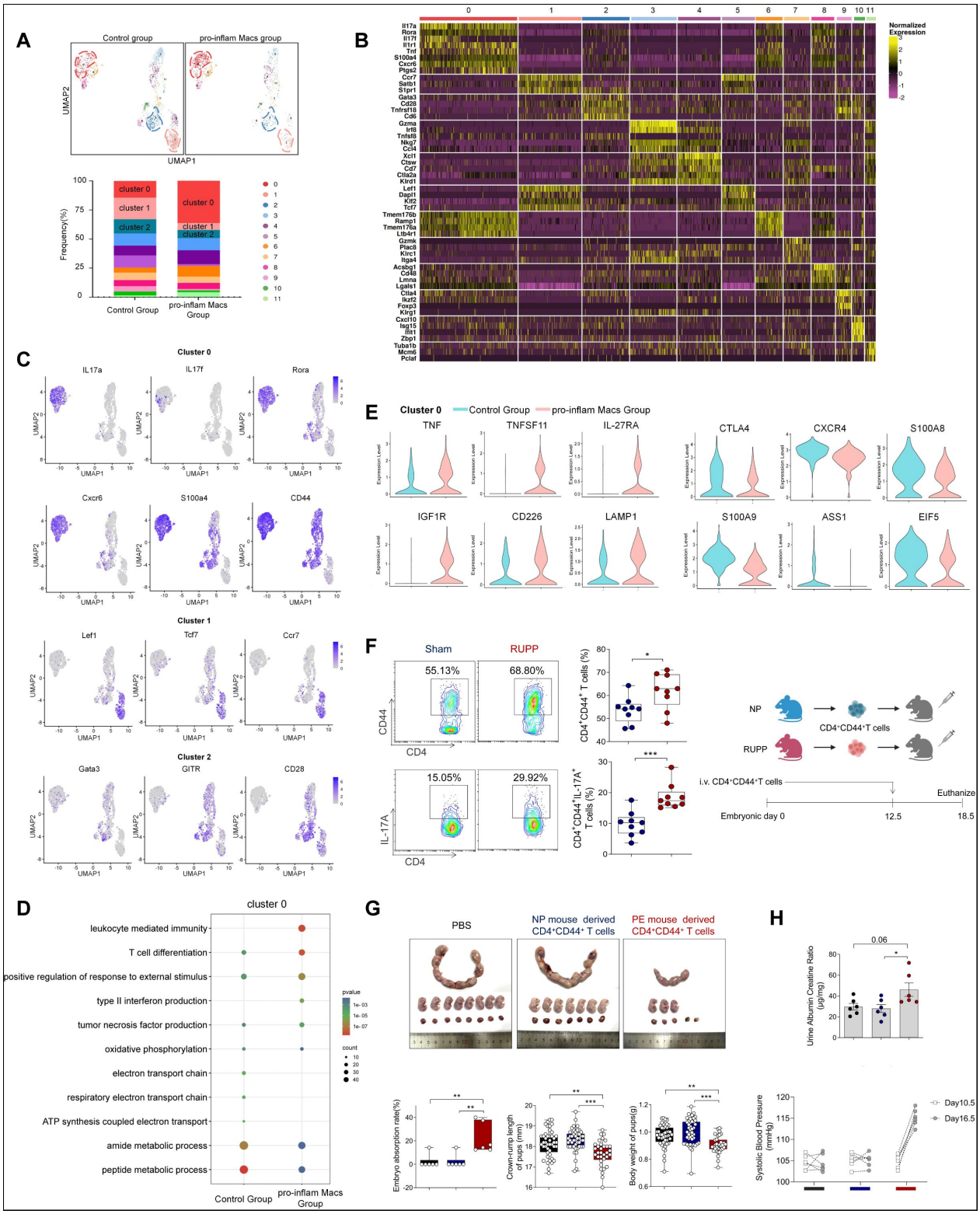
A
Control group
pro-inflam Macs group
UMAP2
UMAP1
Frequency(%)
cluster 0
cluster 1
cluster 2
Control Group
pro-inflam Macs Group
B
Normalized Expression
C
Cluster 0
IL17a
IL17f
Rora
Cxcr6
S100a4
CD44
Cluster 1
Lef1
Tcf7
Ccr7
Cluster 2
Gata3
GITR
CD28
D
cluster 0
leukocyte mediated immunity
T cell differentiation
positive regulation of response to external stimulus
type II interferon production
tumor necrosis factor production
oxidative phosphorylation
electron transport chain
respiratory electron transport chain
ATP synthesis coupled electron transport
amide metabolic process
peptide metabolic process
pvalue
count
Control Group
pro-inflam Macs Group
E
Cluster 0
Control Group
pro-inflam Macs Group
TNF
TNFSF11
IL-27RA
CTLA4
CXCR4
S100A8
IGF1R
CD226
LAMP1
S100A9
ASS1
EIF5
F
Sham
RUPP
55.13%
68.80%
15.05%
29.92%
CD44
CD4
IL-17A
CD4+CD44+ T cells (%)
CD4+CD44+IL-17A+ T cells (%)
NP
RUPP
CD4+CD44+T cells
i.v. CD4+CD44+T cells
Euthanize
Embryonic day 0
12.5
18.5
G
PBS
NP mouse derived CD4+CD44+ T cells
PE mouse derived CD4+CD44+ T cells
Embryo absorption rate(%)
Crown-rump length of pups (mm)
Body weight of pups(g)
H
0.06
Urine Albumin Creatine Ratio (μg/mg)
Systolic Blood Pressure (mmHg)
Day10.5
Day16.5

Figure 6

Identification of the T/NK cells subsets in mice injected pro-inflam Macs and anti-inflam Macs use sc RNA-seq.

(A) UMAP maps showing the 12 clusters of mouse T/NK cells was listed in the up panel. Bar graph showing the frequencies of clusters of T/NK cells in the two groups of mice was listed in the down panel.

(B) Heatmap showing clustering analysis for markers distinguished 12 different clusters of T/NK cells.

(C) UMAP maps showing the distribution of specific markers of cluster 0, 1 and 2.

(D) Dot plot depicting GO enrichment terms that were significantly enriched in the differentially expressed genes in cluster 0 from the pro-inflam Macs group and the control group.

(E) Violin plot of specific differential gene expression in cluster 0 between the pro-inflam Macs group and the control group.

(F) Frequencies of $CD4^+CD44^+$ T cells and the percentages of IL-$17A^+$ cells in $CD4^+CD44^+$ T cells at the maternal-fetal interface in Sham and RUPP group analyzed by flow cytometry.

(G) The embryo abortion rate of pregnant mice, body weight, and crown-rump length of pups measured on day 18.5 of gestation in mice injected PBS, Sham mouse-derived or RUPP mouse-derived $CD4^+CD44^+$ T cells. Black represents mice injected with PBS (n=6); blue represents mice injected with Sham mouse-derived $CD4^+CD44^+$ T cells (n=6); red represents mice injected with RUPP mouse-derived $CD4^+CD44^+$ T cells (n=6).

(H) SBP and UACR of pregnant mice injected with PBS, Sham mouse-derived or RUPP mouse-derived $CD4^+CD44^+$ T cells.

Changes in gene expression patterns of cluster 0 (memory-like Th17 cells) were analyzed in the pro-inflam Macs group and Control group. We found that in the pro-inflam Macs group, enriched GO terms including 'positive regulation of response to external stimulus' and 'tumor necrosis factor production', in which highly express genes such as TNFSF11, TNF, IL27RA, IGF1R, CD226, LAMP1 (**Figure 6C**, **6D**). The control group showed elevated expression of ASS1, EIF5, S100A9, CTLA4, S100A8 and CXCR4; these genes were enriched in GO terms including 'regulation of programmed cell death' and 'cellular biosynthetic process' (**Figure 6D**, **6E**).

Combining the CyTOF and sc-RNA seq data, we found the frequency of memory-like IL-$17A^+CD4^+$ T cells significantly increased at the maternal-fetal interface of individuals with PE. To confirm the effect of memory-like Th17 cells in PE, we constructed an animal model of PE by reducing uterine perfusion pressure (RUPP), and mice with sham operation were considered as controls (**Figure 6-figure supplement 1A**). We found that mice of PE showed an increased embryo absorption rate, decreased fetal weight, and pup crown-rump length compared with the sham operation group (**Figure 6-figure supplement 1B**). Increased systolic blood pressure (SBP) and urine albumin creatine ratio (UACR) were also observed in mice with RUPP, which indicated a successful PE mice mode was built (**Figure 6-figure supplement 1C**). Our studies revealed that the frequency of memory-like Th17 cells ($CD4^+CD44^+$IL-$17A^+$ T cells) was significantly increased in the PE mice (**Figure 6F**).

To confirm the importance of memory-like $CD4^+$ T cells in the pathogenesis of PE, the $CD4^+CD44^+$ T cells in the uterus and placentas from PE or NP mice were sorted and intravenously injected the cells into normal pregnant mice on day12.5 of gestation (**Figure 6F**). Increased embryo

absorption rate, decreased fetal weight and pup crown-rump length were found in mice injected with PE mouse-derived $CD4^+CD44^+$ T cells (**Figure 6G**). The typical PE-like symptoms, including increased SBP and UACR, were also observed in those mice (**Figure 6H**).

It has been reported that sustained expansion of immunosuppressive memory Tregs during prior pregnancy is beneficial for maintaining a second pregnancy (Rowe et al., 2012). To verify whether memory-like Th17 cells promote the recurrence of PE, we established a second pregnant mouse model with a history of PE or NP in the first pregnancy. An increased embryo resorption rate, decreased crown-rump length, and fetal weight were found in mice with a history of PE pregnancy compared with those with a history of NP pregnancy (**Figure 6—figure supplement 1D**). Moreover, mice with a history of PE in the first pregnancy showed increased SBP and UACR during the second pregnancy (**Figure 6—figure supplement 1E**). Consistently, higher levels of IL-17A were also found in memory-like $CD4^+$ T cells in mice with a history of PE in the first pregnancy (**Figure 6—figure supplement 1F**).

Therefore, pro-inflam Macs induced the $IL\text{-}17a^+IL17f^+Rora^+Il1r1^+TNF^+Cxcr6^+S100a4^+$ $CD44^+$ memory-like Th17 cells, which was associatied with the development and recurrence of PE.

Pro-inflam Macs lead to a reduced proportion of gDMSCs

The uterine granulocytes from mice that were transferred with pro-inflam Macs from the uterus and placentas of PE mice were further analyzed using sc RNA-seq. Granulocytes were identified into 12 clusters defined by marker set signatures (**Figure 7A**, **7B**).We found that cluster 0-cluster 3 were different between the two groups: the frequency of cluster 0 and cluster 2 were increased in mice injected with pro-inflam Macs, while the frequency of cluster 1 and cluster 3 were decreased (**Figure 7A**). Cluster 0 has the signature of a mature granulocyte (FOS, FOSB) (Montaldo et al., 2022), and also highly expresses IL-1R2 and CSF3R; Cluster 1 highly express genes associated with immunoregulation genes (Hmox1, CCL4, CCL3, Lcn2) (Wenzel et al., 2022; Montaldo et al., 2022); Cluster 2 highly expressed pro-inflammatory genes (IFITM1, IL1B, Ptgs2, Cxcl3) (Ulff-Møller et al., 2018; Drummond al., 2022); while cluster 3 highly expressed gMDSCs associated genes (Ly6g, S100a8, S100a9, Retnlg, Wfdc21) (von Wulffen et al., 2023; Kao al., 2023) (**Figure 7C**). Our animal experiments above (**Fig 4**) have identified a reduced proportion of $CD11b^+Ly6G^+$ gMDSCs in the mice injected with pro-inflam Macs. Changes in gene expression patterns of cluster 3 (gMDSCs) were analyzed in the pro-inflam Macs group and the control group. Enriched GO terms including 'tumor necrosis factor production' and 'leukocyte mediated immunity' were found in the pro-inflam Macs group, which highly express the genes such as IRF7, EGR1, C1QA, C1QB, CCL2, CSF3R, TNFRSF1B (**Figure 7D**, **7E**). The control group showed elevated expression of CCL4, CXCL10, CD177, MMP8, S100A13, LCN2 and SPP1; these genes were enriched in 'granulocyte migration' and 'localization' ((**Figure 7D**, **7E**).

In conclusion, from the rodent experiments and the data of scRNA-seq, we demonstrated that pro-inflam Macs suppressed the production of $Ly6g^+S100a8^+S100a9^+Retnlg^+Wfdc21^+$ gMDSCs.

Pro-inflam Macs induced the production of memory-like Th17 cells via IGF1-IGF1R

Our results above showed that pro-inflam Macs induced memory-like Th17 cells in PE, however, the underlying molecular mechanisms were still unknown. CellPhoneDB analysis indicated that increased communication counts and signaling pathways numbers between macrophages and T/NK cells were observed in mice injected with pro-inflam Macs (**Figure 8—figure supplement 1A, 1B**). Then we identified the interacting ligand-receptor pairs between different types of immune cells and macrophages. Insulin-like growth factor 1 (IGF1) -IGF1 receptor (IGF1R) ligand-receptor pair was significantly enhanced between macrophages and T/NK cells in mice injected with pro-inflam Macs (**Figure 8A**). IGF1 has significant effects on immune function maintenance, and signaling through IGF1R could cause increased aerobic glycolysis, favoring Th17 cell

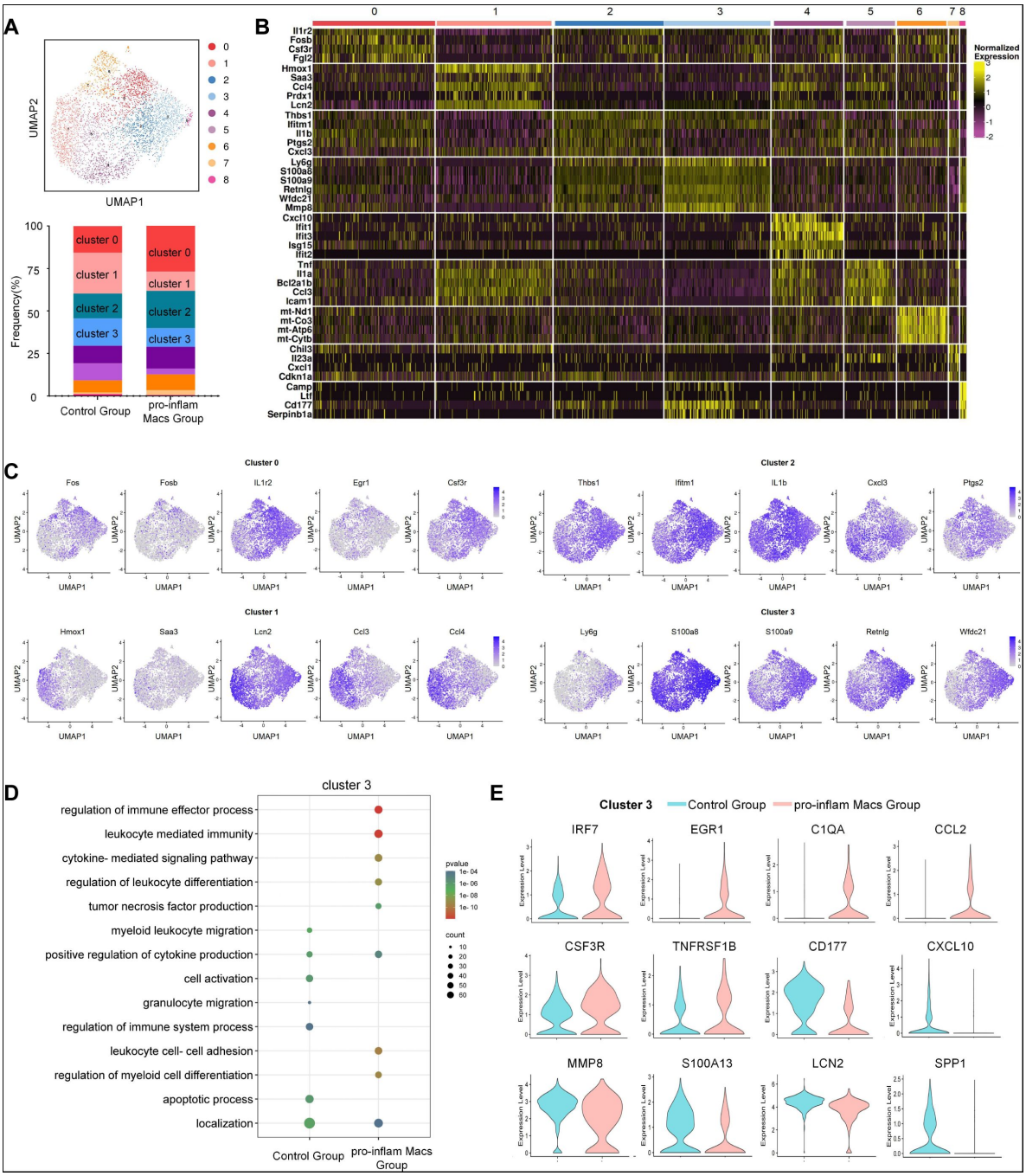

Figure 7

Identification of the granulocytes subsets in mice injected pro-inflam Macs and anti-inflam Macs use sc RNA-seq.

(A) UMAP maps showing the 9 clusters of mouse granulocytes was listed in the up panel. Bar graph showing the frequencies of clusters of granulocytes in the two groups of mice was listed in the down panel.
(B) Heatmap showing clustering analysis for markers distinguished 9 different clusters of granulocytes cells.
(C) UMAP maps showing the distribution of specific markers of cluster 0, 1, 2 and 3.
(D) Dot plot depicting GO enrichment terms that were significantly enriched in the differentially expressed genes in cluster 3 from the pro-inflam Macs group and the control group.
(H) Violin plot of specific differential gene expression in cluster 3 between the pro-inflam Macs group and the control group.

differentiation over that of Treg cells (Bekkering et al., 2018; DiToro et al., 2020). For further demonstration, we analyzed the frequencies of $IGF1^{+}CD14^{+}$ cells and $IGF1R^{+}CD4^{+}$ cells in placentas of individuals with PE and NP and found them significantly increased in the PE group (**Figure 8B**).

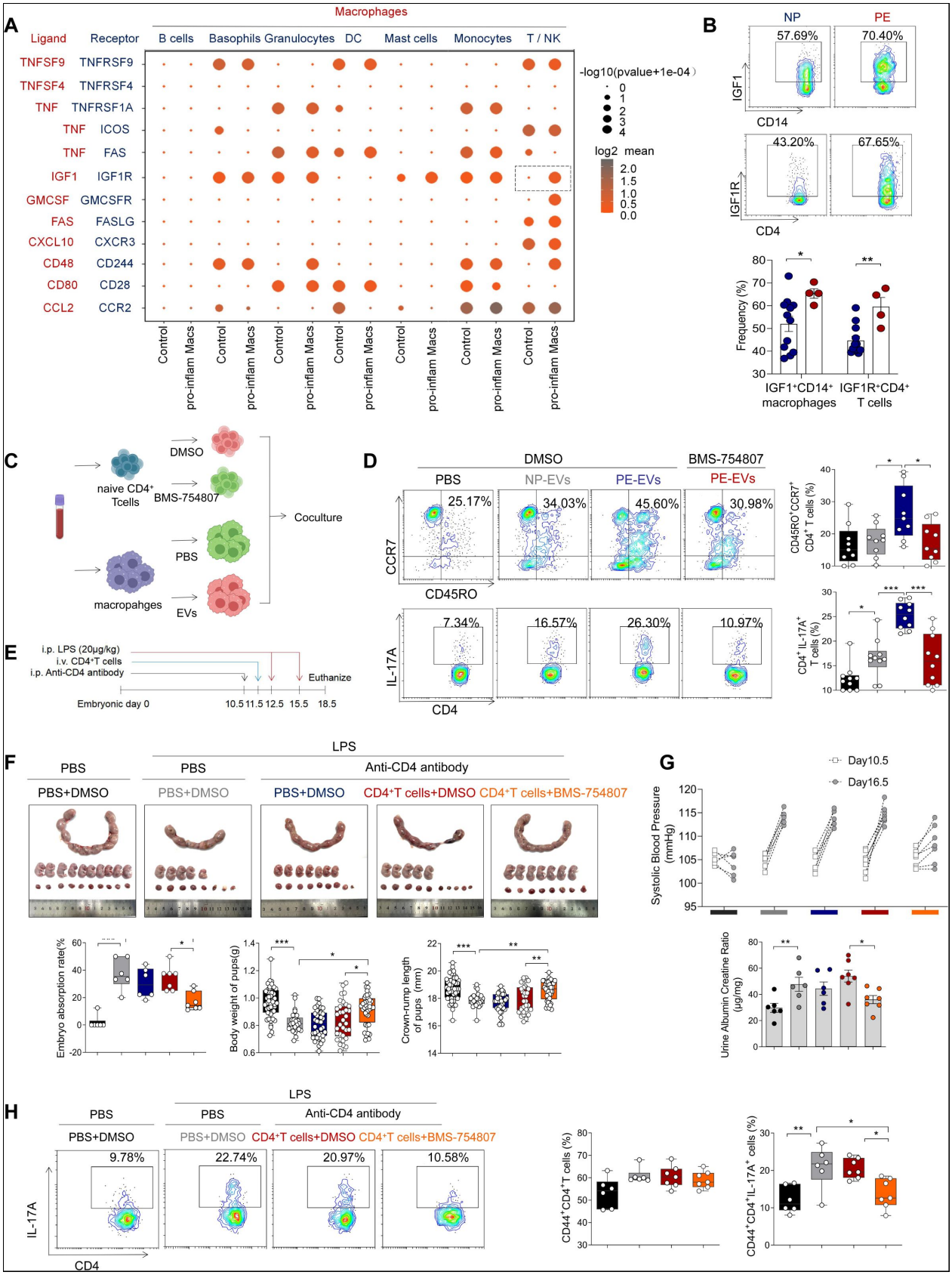
A
Macrophages
Ligand
Receptor
B cells
Basophils
Granulocytes
DC
Mast cells
Monocytes
T / NK
TNFSF9 TNFRSF9
TNFSF4 TNFRSF4
TNF TNFRSF1A
TNF ICOS
TNF FAS
IGF1 IGF1R
GMCSF GMCSFR
FAS FASLG
CXCL10 CXCR3
CD48 CD244
CD80 CD28
CCL2 CCR2
Control
pro-inflam Macs
-log10(pvalue+1e-04)
log2 mean
B
NP
PE
57.69%
70.40%
IGF1
CD14
43.20%
67.65%
IGF1R
CD4
Frequency (%)
IGF1+CD14+ macrophages
IGF1R+CD4+ T cells
C
naive CD4+ Tcells
macropahges
DMSO
BMS-754807
PBS
EVs
Coculture
D
DMSO
BMS-754807
PBS
NP-EVs
PE-EVs
PE-EVs
25.17%
34.03%
45.60%
30.98%
CCR7
CD45RO
CD45RO+CCR7+ CD4+ T cells (%)
7.34%
16.57%
26.30%
10.97%
IL-17A
CD4
CD4+ IL-17A+ T cells (%)
E
i.p. LPS (20μg/kg)
i.v. CD4+T cells
i.p. Anti-CD4 antibody
Euthanize
Embryonic day 0
10.5 11.5 12.5 15.5 18.5
F
LPS
PBS
PBS
Anti-CD4 antibody
PBS+DMSO
PBS+DMSO
PBS+DMSO
CD4+T cells+DMSO
CD4+T cells+BMS-754807
Embryo absorption rate(%
Body weight of pups(g)
Crown-rump length of pups (mm)
G
Day10.5
Day16.5
Systolic Blood Pressure (mmHg)
Urine Albumin Creatine Ratio (μg/mg)
H
LPS
PBS
PBS
Anti-CD4 antibody
PBS+DMSO
PBS+DMSO
CD4+T cells+DMSO
CD4+T cells+BMS-754807
9.78%
22.74%
20.97%
10.58%
IL-17A
CD4
CD44+CD4+T cells (%)
CD44+CD4+IL-17A+ cells (%)

Figure 8

Pro-inflam Macs induce the generation of memory-like Th17 cells via IGF1-IGF1R

(A) Signaling modules indicated by ligand-receptor pairing between macrophages and other types of immune cells at the maternal-fetal interface using CellPhoneDB.

(B) Frequencies of $IGF1^{+}CD14^{+}$ cells and $IGFIR^{+}CD4^{+}$ cells in placentas of individuals with NP and PE (n=12 in NP group, n=4 in PE group).

(C) Schematic of the experimental workflow to induce memory-like T cells in vitro. Macrophages, after incubating with PBS, NP-EVs or PE-EVs, were co-cultured with $CD4^{+}$ naïve T cells treated with DMSO or BMS-754807. Cells were isolated from human peripheral blood.

(D) Frequencies of $CD45RO^{+}CCR7^{+}$Th17 cells. Black represents $CD4^{+}$ naïve T cells treated with DMSO; gray represents $CD4^{+}$ naïve T cells cocultured with NP-EVs-treated macrophages; blue represents $CD4^{+}$ naïve T cells co-cultured with PE-EVs-treated macrophages; red represents $CD4^{+}$ naïve T cells treated with BMS-754807 before co-cultured with PE-EVs-treated macrophages (n=10 in each group).

(E) Schematic of mice transferred $CD4^{+}$ T cells treated with BMS-754807 or PBS. Anti-CD4 antibody was used to deplete $CD4^{+}$ T cells in mice on day 10.5 of gestation. $CD4^{+}$ T cells were transferred into mice on day 11.5 of gestation. 20 μg/kg lipopolysaccharide (LPS) was intraperitoneally injected on day 12.5 and 15.5 of gestation to induce a PE-like pregnant mice model. Mice were sacrificed on day 18.5 of gestation.

(F) Embryo abortion rate of pregnant mice, body weight and crown-rump length of pups were measured on day 18.5 of gestation. Black represents the control group mice (n=6); gray represents mice treated with LPS (20μg/kg) to construct an animal model of PE (n=6); blue represents anti-CD4 antibody treated PE mice (n=6); red represents anti-CD4 antibody treated PE mice injected with $CD4^{+}$ T cells with DMSO treatment (n=7); orange represents anti-CD4 antibody treated PE mice injected with $CD4^{+}$ T cells with BMS754807 treatment (n=7).

(G) SBP and UACR of pregnant mice in the five groups.

(H) The frequencies of $CD4^{+}$ $CD44^{+}$ $IL\text{-}17A^{+}$ cells analyzed by flow cytometry.

The results were compared using one-way ANOVA and represented as mean±SEM (*P < 0.05, ** P < 0.01, *** P < 0.001; NS, not significant).

Trophoblast-derived extracellular vesicles from the placenta of PE (PE-EVs), which carry the fetal antigen, could induce M1 macrophage polarization to participate in the development of PE according to our previous study (X. Liu et al., 2022). To confirm whether pro-inflammatory macrophages induced the production of memory-like Th17 cells via IGF1-IGF1R, macrophages from human peripheral blood, after incubating with PBS, trophoblast-derived extracellular vesicles from NP (NP-EVs) or PE-EVs in vitro, were co-cultured with $CD4^{+}$ naïve T cells (**Figure 8C**). The frequencies of memory-like $CD45RO^{+}$ $CCR7^{+}$ $IL\text{-}17A^{+}$ $CD4^{+}$ cells significantly increased in the PE-EVs-induced macrophages group rather than in the NP-EVs-induced macrophages group. However, the frequencies of memory-like Th17 cells significantly decreased after $CD4^{+}$ naïve T cells were treated with the IGF1R inhibitor BMS-754807, an inhibitor of IGF1R (**Figure 8D**).

To investigate the role of IGF1-IGF1R in the development of PE in vivo, $CD45^{+}$ $CD4^{+}$ T cells from NP mice were isolated and treated with BMS-754807 or PBS, then injected into NP mice at day 11.5 of gestation (**Figure 8E**). Lipopolysaccharide (LPS)-induced PE mice model was constructed by intraperitoneal injection of LPS on day12.5 and day15.5 of gestation (Han et al., 2021), and anti-

CD4 antibody was used to deplete the $CD4^+$ T cells in pregnant mice. The mice injected with $CD4^+$ T cells treated by BMS-754807 presented decreased embryo resorption rate and increased pup crown-rump length and fetal weight (**Figure 8F**), decreased SBP and UACR (**Figure 8G**), and decreased frequency of memory-like Th17 cells at the maternal-fetal interface (**Figure 8H**). These data suggested that pro-inflam Macs could induce the production of memory-like Th17 via the IGF1-IGF1R, leading to the development of PE.

Discussion

Preeclampsia, a progressive systemic disease during pregnancy, is closely related to the alterations in the immune environment at the maternal-fetal interface. In this study, the overall immune cell profile in the placenta of individuals with NP, PE, GDM and GDM&PE were detected by CyTOF and a PE-specific change in immune microenvironment of maternal-fetal interface were described for the first time. Further, we provided a novel insight that pro-inflam Macs induced memory-like Th17 cells, memory-like $CD8^+$ T cells, and suppressing the production of gMDSCs in mice maternal-fetal interface by scRNA-seq. In addition, we first validated that IGF1-IGF1R was involved in producing memory-like Th17 cells induced by pro-inflammatory macrophages in vitro and in vivo, thus leading to the development of PE.

Various studies represented the effect of a particular subset of immune cells in the pathogenesis of PE or GDM (Bachmayer et al., 2006; Care et al., 2018; Cornelius et al., 2015a; Eghbal-Fard et al., 2019; Faas et al., 2014; Fu et al., 2014; Fukui et al., 2011; Lampé et al., 2015; Lampé et al., 2011; Lang et al., 2021; D. Liu et al., 2021; Lu et al., 2020; Santner-Nanan et al., 2009; Sasaki et al., 2007; Travis et al., 2020; Yao et al., 2019). However, only one report has provided an overall analysis of immune cells in the human placental villi in the presence and absence of spontaneous labor at term by scRNA-seq (Miller et al., 2022). Here we used CyTOF and scRNA-seq to comprehensively analyze the immune cell profile and explore the interaction of immune cells in PE. Additionally, most previous studies have studied immune cells from maternal systemic circulation rather than directly from the tissue of maternal-fetal interface (Cornelius et al., 2015b; Deer et al., 2021; Santner-Nanan et al., 2009; Shields et al., 2018; Wallace et al., 2012). In this study, cells were directly isolated from the tissue of maternal-fetal interface, which is considered as a more accurate approach to mimic the real immune environment of the maternal-fetal interface.

Abnormal inflammatory responses were reported to play an important role in the pathogenesis of both PE and GDM (Aneman et al., 2020; Corrêa-Silva et al., 2018; Deer et al., 2023; Jung et al., 2022; McElwain et al., 2021). However, It is unclear how the maternal-fetal interface immune microenvironment differs between the two diseases. We analyzed the overall placental immune cell profile in NP, PE, GDM and GDM&PE by CyTOF and revealed a PE-specific immune cell profile: The frequencies of memory-like Th17 cells ($CD206^-CD163^-CD38^{mid}CD107a^{low}CD86^{mid}$HLA-$DR^{mid}CD14^+$) were increased, while the decreased frequencies of $CD69^{hi}$Helios $^{mid}CD127^{mid}$ γδT cells, anti-inflam Macs ($CD206^+CD163^-CD86^{mid}CD33^+$HLA-$DR^+$) and granulocyte myeloid-derived suppressor cells (gMDSCs, $CD11b^+CD15^{hi}$HLA-DR^{low}) were observed in the placenta of PE, but not in that of GDM or GDM&PE compared with that of NP.

PE is often divided into two subtypes based on the time of onset. Late-onset PE, occurring at 34 weeks of gestation or later, accounts for most preeclampsia cases, while early-onset PE, occurring before or at 33 weeks of gestation(Lisonkova and Joseph, 2013). However, our previous study observed no significant difference in the M1/M2 macrophage polarization in placentas with early-onset or late-onset PE (X. Liu et al., 2022). Therefore, our research was conducted regardless of the preeclampsia-onset type to ensure consistency in macrophage polarization of the two subtypes.

There have been studies indicating that macrophages, Th17 cells, Treg cells, and $CD8^+$ T cells play an essential role in PE development (Care et al., 2018; Eghbal-Fard et al., 2019; Lager et al., 2020; Yao et al., 2019). Macrophages was indicated with a pro-inflammatory phenotype in the placenta with PE (Faas et al., 2014; Yao et al., 2019). Care et al. reported that placental Tregs helped suppress inflammation at the maternal-fetal interface (Care et al., 2018). Similarly, Lu et al. found an abnormal increase of IL-17A in the placenta in the development of PE (Lu et al., 2020). Meanwhile, the abnormal infiltration of $CD8^+$ T cells in the placenta may contribute to PE (Lager et al., 2020). Consistent with the previous findings, we found that memory-like $CD4^+$ and memory-like $CD8^+$ T cells significantly increased in the PE group and that IL-17A was significantly higher expressed in $CD4^+$ memory-like T cells from the PE group, which is vital in vascular inflammation, leading to the development of PE (Amador et al., 2014; Madhur et al., 2021). Though memory T cells play a key role in fetal-maternal tolerance in normal pregnancy (Kieffer et al., 2019), few studies have reported the characteristics of memory-like T cells in the development of PE.

We constructed an adoptive transferred mouse model and confirmed that pregnant mice developed PE symptoms after transferring PE mouse-derived memory-like $CD4^+$ T cells. It is worth noting that we isolated $CD4^+$ memory-like T cells directly from the maternal-fetal interface, which is different from previous studies that the $CD4^+$ T cells for adoptive transfer were isolated from the spleen and induced in vitro (Cornelius et al., 2015b; Deer et al., 2021; Shields et al., 2018; Wallace et al., 2012). Recurrence is an important concern in individuals with PE (Bernardes et al., 2019). We found that a prior PE pregnancy increased the probability of PE in the next pregnancy in mice, accompanied by an increased frequency of memory-like Th17 cells at the maternal-fetal interface, suggesting that increased memory-like Th17 cells are positively related to the recurrence of PE. However, additional animal experiments are needed to confirm the function of the fetal-specific memory Th17 cells in the recurrence of PE. Activation of $CD8^+$ T cells and Th1 cells can be induced by abnormal polarized macrophages in recurrent miscarriage (Li et al., 2022). gMDSCs have been reported to have immune suppressive activity and are necessary for maintaining maternal-fetal tolerance (Köstlin-Gille et al., 2019; Zhou et al., 2018). However, the correlation between macrophages and other immune cells in the development of PE remained unclear. We verified that pro-inflam Macs induced memory-like Th17 cells and memory-like $CD8^+$ T cells and inhibited the production of gMDSCs in PE by correlation analysis and adoptive transfer in animal experiments for the first time, indicating that the immune cells orchestrate a network in the maternal-fetal interface elaborately.

The function of IGR1 and IGF1R in PE is controversial. IGF1 plays a significant role in maintaining immune function, and IGF1R facilitates the differentiation of naïve $CD4^+$ T cells into Th17 cells (DiToro et al., 2020). A study showed that IGF-1R was downregulated in the serum of individuals with PE (Liao et al., 2021). Decreased amounts of IGF1R were also found in the placentas of individuals with PE (Robajac et al., 2015). However, another study found no significance in the affinity and the number of IGF-1R between placentas from individuals with PE or not (Díaz et al., 2005). We found that mice exhibiting PE symptoms had significantly enhanced IGF1-IGF1R interaction between inflammatory macrophages and memory-like Th17 cells by analyzing the data of scRNA-seq. Then, this finding was further confirmed in human placentas from individuals with PE and NP, for the frequencies of $IGF1^+$ $CD14^+$ cells and $IGF1R^+$ $CD4^+$ cells were found to significantly increase in the PE group. In vitro, we found that PE-EVs-treated macrophages secreted more IGF1 than NP-EV-treated macrophages and induced a higher frequency of memory-like Th17 cells. The inhibition of IGF1R on $CD4^+$ naïve T cells resulted in a decreased frequency of memory-like Th17 cells, implying that the IGF1-IGF1R is critical for the production of memory-like Th17 cells induced by inflammatory macrophages. Animal experiments confirmed that IGF1R inhibition on $CD4^+$ T cells at the maternal-fetal interface reduced the frequency of memory-like Th17 cells, improving PE.

In addition, placentas from different groups for CyTOF analysis and flow cytometry were matched by age, preterm pregnancies, and previous abortions; however, there are differences in body mass index (BMI), gestational age, term pregnancies, and the number of living children. Obesity can increase inflammatory and oxidative stress markers in the placental environment (Spradley et al., 2015). Also, it has been reported that the placental immune state shifts with gestational age (Lewis et al., 2018). However, as PE is often accompanied by obesity and early termination of pregnancy, it is difficult to exclude these factors in sample collection. Moreover, limited placental samples in the GDM&PE group are the shortage of this study, for it is hard to collect enough clean samples that exclude interference factors because the number of pregnant women exposed to COVID-19 has increased sharply since December 2022 in China.

In summary, this study demonstrated the statistically distinguished placental immune microenvironment in individuals with PE, but not in those with GDM or GDM&PE. More importantly, macrophages orchestrate a network in the maternal-fetal interface elaborately. These findings provide novel insights into PE pathogenesis and a potential immune target for the clinical prevention and treatment of PE.

Materials and Methods

Clinical sample collection

The samples used in this study were collected from Sir Run Run Shaw Hospital between October 2020 and August 2023. Informed consent was obtained from all volunteers, and the Ethics Committee of Sir Run Run Shaw Hospital, Zhejiang University School of Medicine, approved the study. Human placentas were obtained from women with NP, PE, GDM, or GDM&PE who underwent elective cesarean delivery. The diagnostic criteria for PE included new-onset hypertension after 20 weeks of gestation with SBP ≥140 mmHg and/or diastolic blood pressure ≥90 mmHg and proteinuria (≥300 mg) on at least two occasions. A positive glucose tolerance test diagnoses gestational diabetes mellitus. Women with normal blood pressure, full-term pregnancies, and no complications were designated as controls. The detailed clinical characteristics of the pregnant women in this study are presented in **Table 5** and **Table 6**.

Mice

Eight-week-old female C57 mice and ten-week-old male BALB/c mice were purchased from Hangzhou Ziyuan Laboratory Animal Technology Co., Ltd (Hangzhou, China) and Shanghai Jihui Experimental Animal Breeding Co., Ltd (Shanghai, China), respectively. All animals were maintained under pathogen-free conditions. The Guide for the Care and Use of Laboratory Animals (China) conducted all experimental procedures involving animals, and the Animal Research Ethics Committee of the Sir Run Run Shaw Hospital of Zhejiang University approved the protocols.

Female C57 mice were mated with male BALB/c mice to establish an allogeneic pregnancy model (Rowe et al., 2012). The day of the vaginal plug detection was considered day 0.5 of pregnancy. SBP was measured using a noninvasive mouse tailcuff BP analyzer (BP-2010A, Softron, Japan) at 12.5, and 16.5 days of gestation. Three random urine samples were collected after day 16.5 of gestation, and UACR was measured by urinary microalbumin (CH0101060, Maccura, China). Mice were euthanized on day 18.5 of gestation.

Table 5

Details of the individual with NP or PE included in the study

Parameters	NP (n=30)	PE (n=30)	p Value
Age (years)	31.13 ± 2.9747	31.50 ± 4.1693	0.0741
BMI (kg/m^2)	27.24 ± 2.8048	29.48±3.9295	0.0155
Gestational age (weeks)	38.68± 0.6038	35.53 ± 3.29	<0.0001
Number of living children	0.6000 ± 0.4900	0.4667 ± 0.6182	0.3665

Table 6

Details of the individual with early-onset preeclampsia or late-onset preeclampsia included in the study

Parameters	Early-onset preeclampsia(n=11)	Late-onset preeclampsia (n=19)	p Value
The gestational week when blood pressure begins to rise	28.82± 2.8220	36.05± 1.129	< 0.0001
Age (years)	32.45± 4.6768	32.36± 3.8472	0.9568
BMI (kg/m^2)	29.64± 2.6840	28.71±4.4506	0.5388
Gestational age (weeks)	33.45± 3.7887	36.77± 1.2171	0.0014
Number of living children	0.36± 0.5045	0.36 ± 0.4956	0.98

Reduction in uterine perfusion pressure mouse model

To construct a mouse model of PE, we ligate uterine arteries in pregnant mice on day 12.5 of gestation. Briefly, after 4% chloral hydrate was intraperitoneal injected for anesthesia, bilateral incisions were made on the back of the pregnant mice, and surgical sutures were used to reduce the blood flow of the bilateral uterine arcades.

Isolation of single cells from the mouse uterus and human placenta

Uterus from pregnant mice and placentas from volunteers were washed twice with ice-cold PBS and cut into small pieces. The tissues were digested with collagenase type IV (1 mg/ml, Sigma-Aldrich, USA) and DNase I (0.01 mg/ml, Sigma-Aldrich, U.S.A) in RPMI 1640 medium (Thermo Fisher Scientific) for 40 min at 200 rpm and 37 °C. The suspensions were strained through 70-μm nylon mesh and centrifuged at 500×g for 5 minutes. Leaving the supernatants, the cell pellets from human placentas need an extra purification by Ficoll (P4350, Solarbio, China) according to the manufacturer's instructions. Human $CD4^+$ memory T cells were isolated using a Human Central and Effector Memory $CD4^+$ T Cell Isolation Kit (17865, STEMCELL, Canada).

Adoptive transferred mouse model

Endogenous macrophages or $CD4^+$ T cells were depleted by injecting PLX3397 (S7818, Selleck, USA), clodronate liposomes (40337ES08, YEASEN, China) or anti-CD4 antibody (BE0003-1, BioXcell, USA) intraperitoneally every three days starting from day 10.5 of gestation.

For the adoptive transferred mouse model, phycoerythrin-conjugated anti-mouse CD4 (12-0041-82, eBioscience, USA) and Pc5.5-conjugated anti-mouse CD44 (45-0441-82, eBioscience, USA) were used to label $CD4^+$ memory-like T cells from uterus and placentas. PE-conjugated anti-mouse CD45 (E-AB-F1136D, Elabscience, China), FITC-conjugated anti-mouse F480 (11-4801-82, eBioscience, USA), and PE-Cyanine7-conjugated anti-mouse CD206 (141719, Biolegend, USA) were used to label anti-inflam Macs from uterus and placentas, and the remaining $CD45^+F480^+CD206^-$ cells were considered pro-inflam Macs. The MoFlo Astrios EQ FACS Cell Sorter at Core Facilities, ZheJiang University School of Medicine (China), was used to obtain specific cells with a purity of > 96%. Briefly, 2–5 × 10^5 $CD4^+$ $CD44^+$ T cells, 5×10^5 pro-inflam Macs, or 5×10^5 anti-inflam Macs were injected to pregnant C57 mice intravenously at day 12.5 of gestation.

2–5 × 10^5 $CD45^+CD4^+$ T cells from uterus and placentas of pregnant mice were sorted and transferred to pregnant C57 mice at day 11.5 of gestation after treating with 100nM BMS-754809 (HY10200; MedChemExpress; USA) or PBS for three days in vitro.

Mass cytometry by time of flight

7 × 10^5 cells from NP (n=9), PE (n=8), GDM (n=8), GDM&PE (n=7) presented in **Table 1** were stained for cell surface markers for 30 min at 4°C in staining medium (PBS containing 1% BSA and 0.02% NaN_3). Cells were washed with protein-free PBS, stained with 2.5 μM cisplatin for 5 min at 25°C and fixed using transcription factor buffer set (BD Biosciences), followed by intracellular staining for 60 min at 4 °C. Then the cells were washed and stored at 4 °C until acquisition. Finally, cells were analyzed on a CyTOF mass spectrometer (Fluidigm, South San Francisco, CA, USA). The data were normalized for each experiment using EQ four-element calibration beads (Fluidigm) and the reference EQ passport P13H2302.

RNA sequencing

5×10^5 $CD45^+F4/80^+CD206^-$ pro-inflam Macs (n=3) and 5×10^5 $CD45^+F4/80^+CD206^+$ anti-inflam Macs (n=3) were isolated from the uterus and placentas of mice with RUPP and high throughput sequencing and bioinformatics analyses were conducted at Shenzhen Huada Gene Technology Service Co. Ltd.(Shenzhen, China). Only differential genes with more than two-fold change and a corrected P value less than 0.05 were considered statistically significant.

Single-cell RNA sequencing (scRNA-seq)

Mice were injected with 5×10^5 $CD45^+F4/80^+CD206^-$ pro-inflam Macs or 5×10^5 $CD45^+F4/80^+CD206^+$ anti-inflam Macs at 12.5 days of gestation and euthanized on day 18.5 of gestation. $CD45^+$ immune cells from the uterus and placenta were isolated from mice transferred pro-inflam Macs and anti-inflam Macs. scRNA-seq was conducted at PLTTECH Service Co. Ltd. (Hangzhou, China). Differential genes with a corrected $P < 0.05$ were considered statistically significant.

Isolation of NP-EVs and PE-EVs

NP-EVs and PE-EVs were isolated and identified using our published protocols (Jiang et al., 2021; X. Liu et al., 2022). Briefly, after digesting the placental tissues from NP or PE, the suspensions were filtered through 100-μm nylon mesh and centrifugated at 3,000×g for 15 minutes. Then the supernatants were filtered with a 0.22-μm filter and centrifuged at 100,000×g for 1h at 4 °C. Then the pellets of EVs were resuspended and centrifuged at 100,000×g once again. A BCA assay kit conducted Protein quantitation of EVs (23235, Thermo Fisher Scientific). To isolate the T-EVs, 500 μg of the EVs were incubated with 1 μg placental alkaline phosphatase antibody (SC-47691, Santa Cruz Biotechnology) at 4 °C overnight, then washed in the recommended buffer (PBS containing 2% exosome-free FBS and 1 mmol/L ethylenediaminetetraacetic acid), and centrifuged at 100 000×g for 1 hour at 4 °C. After resuspended, the total EVs were sorted by EasySep Mouse PE Positive Selection Kit II (17666, STEMCELL) to collect the final NP-EVs or PE-EVs.

Induction of $CD4^+$ memory-like T cells

Macrophages were obtained after five days of culture of mononuclear cells isolated from human peripheral blood following previous protocols (X. Liu et al., 2022). NP-EVs or PE-EVs in a 50 μg/mL concentration were added to macrophages and co-cultured at 37 °C for 8 h. The human $CD4^+$ naïve T cells Isolation Kit (19555, STEMCELL, Canada) was used to isolate purified $CD4^+$ naïve T cells from human peripheral blood cells according to the manufacturer's instructions. Then, $CD4^+$ naïve T cells were co-cultured with EV-treated macrophages for six days. Flow cytometry was performed to measure the frequency of memory-like Th17 cells. For animal experiments, $CD4^+$ naïve T cells sorted from the uterus and placentas of pregnant mice were cultured with the IGF1R inhibitor BMS-754807 at a concentration of 10 μM for three days before co-cultured with macrophages.

Flow cytometry

Single immune cells from the mice uterus were obtained following the method described above. After incubation with Cell Stimulation Cocktail (00-4975-93, Invitrogen, USA) for five hours at 37 °C, cells were collected and surface staining for either phycoerythrin-conjugated anti-mouse CD4 (12-0041-82, eBioscience, USA), APC-conjugated anti-mouse CD8 (100711, BioLegend, USA), phycoerythrin-Cy5.5-conjugated anti-mouse CD44 (45-0441-82, eBioscience, USA), APC-conjugated anti-mouse CD11b (101212, BioLegend, USA), FITC-conjugated anti-mouse Gr-1 (108406, BioLegend, USA), PE-Cyanine7-conjugated anti-mouse Ly6G (E-AB-F1108H, elabscience, China) or intracellular staining for 488-conjugated anti-mouse IL-17A (506910, BioLegend, USA) was performed according to the manufacturer's instructions.

Single placental and peripheral lymphocytes and were obtained following the method described above. The Human Central and Effector Memory $CD4^+$ T cell Isolation Kit (17865, STEMCELL, Canada) was used to obtain purified memory $CD4^+$ T cells, according to the manufacturer's instructions. After incubation with Cell Stimulation Cocktail (00-4975-93, Invitrogen, USA) for five hours at 37 °C, cells were collected and surface staining for phycoerythrin-conjugated anti-human CD4 (2384240, eBioscience, USA), FITC-conjugated anti-human CD45RO (304204, BioLegend, USA), and phycoerythrin-Cy7-conjugated anti-human CCR7 (353227, BioLegend, USA) or intracellular staining for APC-conjugated anti-human IL-17A (17-7179-42, eBioscience, USA) and Foxp3 (320014, BioLegend, USA) was performed according to the manufacturer's instructions.

Immunofluorescence

Frozen sections of the placentas were permeabilized with PBS containing 0.5% Triton X-100 (PBST) for 20 min and incubated for 1 h with a blocking buffer in PBST. The sections were then incubated with anti-CD4 (sc-1176, Santa Cruz Biotechnology, China) and FITC-conjugated anti-human CD45RO (304204, BioLegend, USA) at 4 °C overnight, followed by Alexa Fluor 568-conjugated secondary antibodies (dilution: 1:200, Yeasen, China) for 1 h. The slides were counterstained with 4,6-diamidino-2-phenylindole (DAPI, 1 μg/ml; Roche, Switzerland) for 20 min. Digital images were obtained using confocal fluorescence microscopy (ZEISS LSM 800, Germany). ImageJ software was used to quantify the fluorescence intensity from immunofluorescence (IF) images.

Statistical analysis

Data were analysed using SPSS version 20. After the Shapiro-wilk test, the data were confirmed to be non-normal distribution. Kruskal-wallis test was used to compare the results of experiments with multiple groups. All data are presented as mean ± SEM (*P < 0.05, ** P < 0.01, *** P < 0.001; NS, not significant).

Acknowledgements

The authors would like to express their heartfelt gratitude to the participants for their contributions. This work was financially supported by the National Natural Science Foundation of China (82271694), the Zhejiang Province Natural Science Foundation key project fund (LZ24H040002), the Zhejiang Medicine and Health Science and Technology Plan Project (2023KY800).

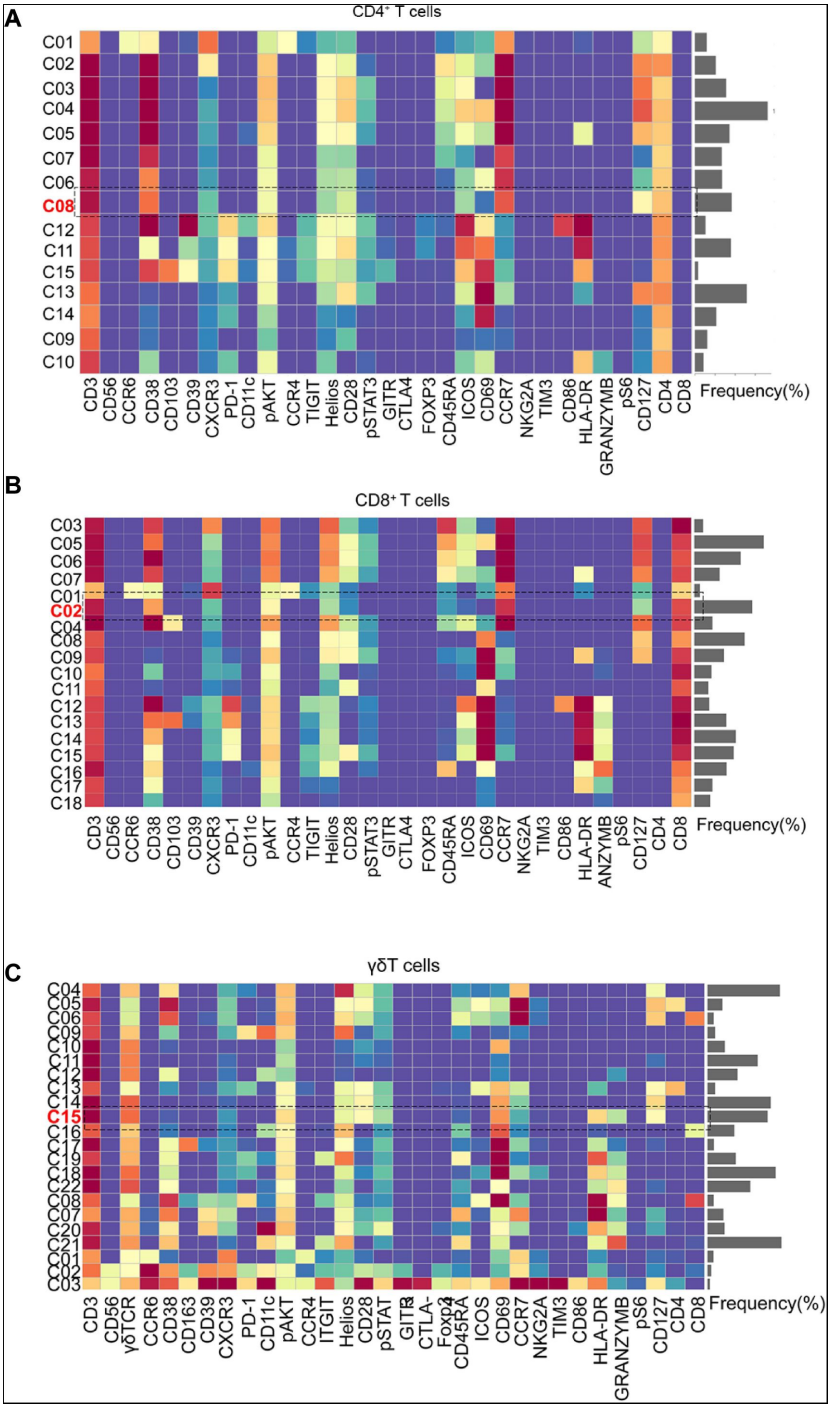

Figure 2—figure supplement 1

Identification of the placental T cell subsets.

(A) Heatmap showing the expression levels of markers in the $CD4^+$ T subsets.
(B) Heatmap showing the expression levels of markers in the $CD8^+$ T cells.
(C) Heatmap showing the expression levels of markers in the γδT cells.

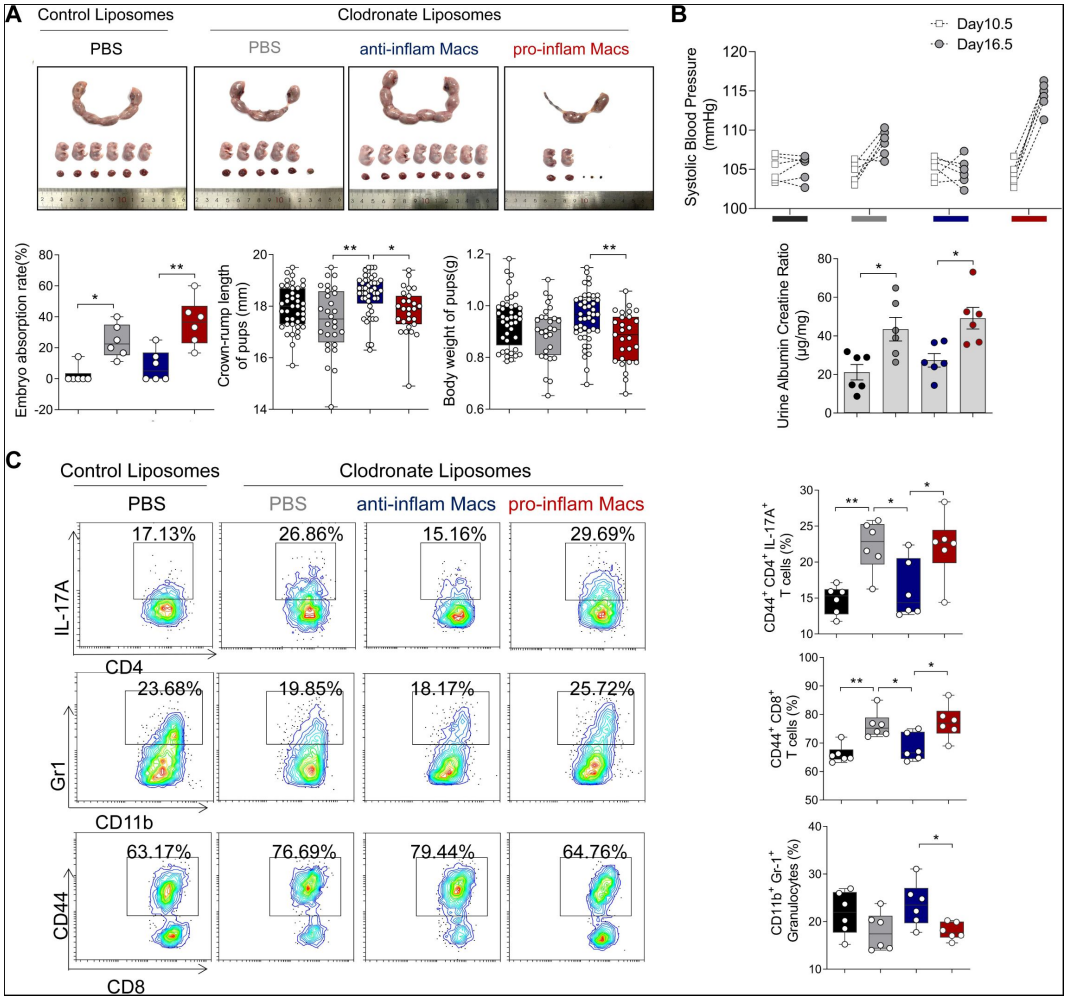

Figure 4—figure supplement 1

Clodronate liposomes were used to used to deplete the macrophages of pregnant mice to demonstrate that pro-inflam Macs lead to immune imbalance.

(A) Embryo abortion rate of the pregnant mice, body weight and crown-rump length of pups measured on day 18.5 of gestation. Black represents mice treated with control liposomes (n=6); gray represents mice treated with clodronate liposomes (n=6); blue represents mice injected with $CD45^+F4/80^+CD206^+$ anti-inflam Macs (n=6); red represents mice injected with $CD45^+F4/80^+CD206^-$ pro-inflam Macs (n=6).
(B) SBP and UACR of pregnant mice in the four groups.
(C) Frequencies of $CD44^+CD4^+IL\text{-}17A^+$ cells, $CD44^+CD8^+$ T cells and $CD11b^+Gr1^+$ granulocytes analyzed by flow cytometry.

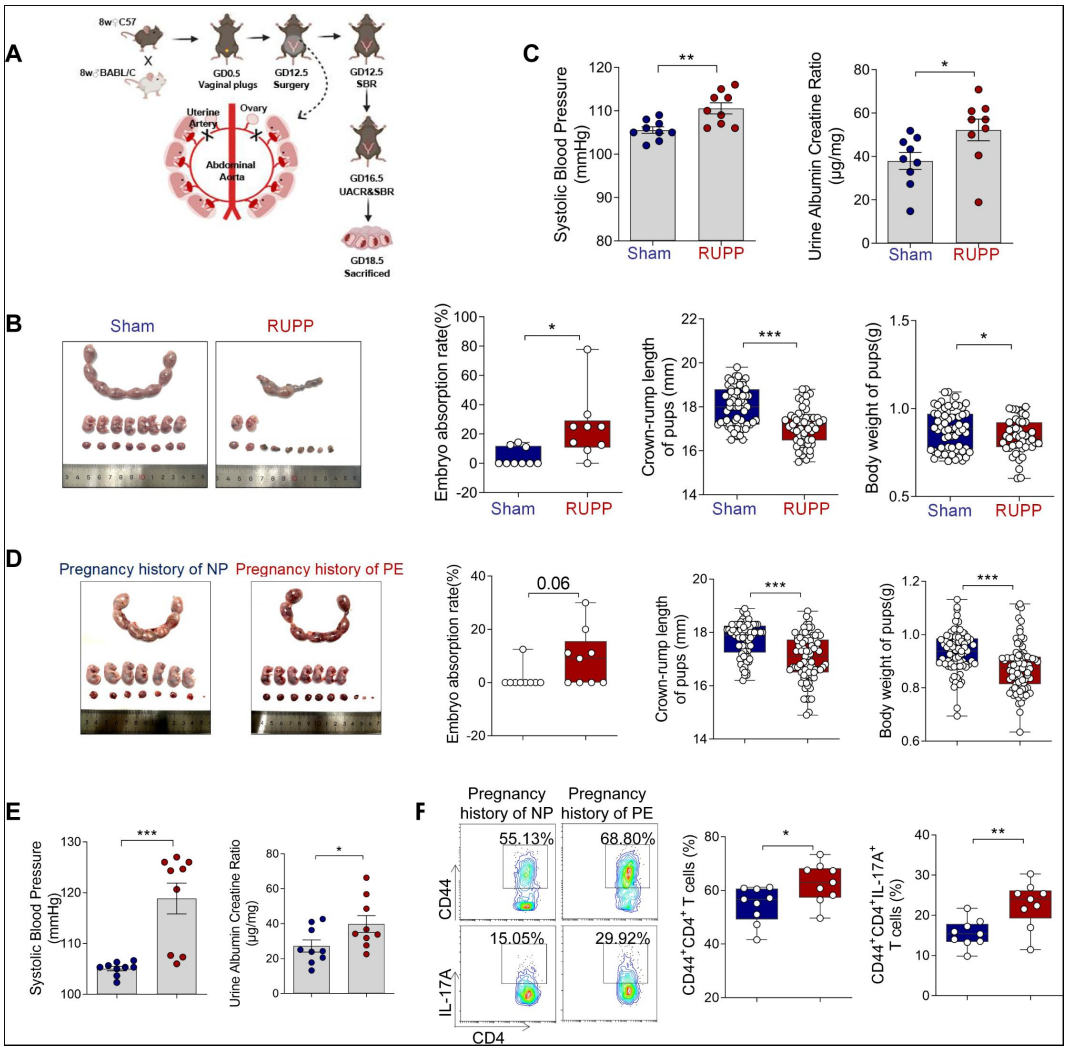

Figure 6—figure supplement 1

Memory-like Th17 cells may be associated with the recurrence of PE.

(A) Experimental design of mice model with PE by reducing uterine perfusion pressure (RUPP) on day 12.5 of gestation. Mice with sham operation were considered as controls. Systolic blood pressure (SBP) and urine albumin creatine ratio (UACR) were measured on day 12.5 and 16.5 of gestation respectively. Mice were sacrificed on day 18.5 of gestation.
(B) The embryo abortion rate of pregnant mice, body weight, and crown-rump length of pups measured on day 18.5 of gestation in the Sham and RUPP group. Embryo abortion rate = number of absorbed embryos/total number of embryos. Blue represents mice in the Sham group (n=9); Red represents mice in the RUPP group (n=9).
(C) SBP and UACR of pregnant mice in Sham and RUPP group.
(D) Embryo abortion rate of pregnant mice, body weight and crown-rump length of pups measured on day 18.5 of gestation. Black represents mice with previous normal pregnancy (n=9); gray represents mice with previous pregnancy with PE (n=9).
(E) SBP and UACR of second pregnant mice with a history of PE or NP in the first pregnancy measured on day 16.5 of gestation.
(F) Frequencies of $CD4^+$ $CD44^+$ T cells and the levels of IL-17A in $CD4^+$ $CD44^+$ T cells in mice with a pregnancy history with NP and PE analyzed by flow cytometry.
Data were compared using the Student's t-test and represented as mean±SEM (*P < 0.05, ** P < 0.01, *** P < 0.001; NS, not significant).

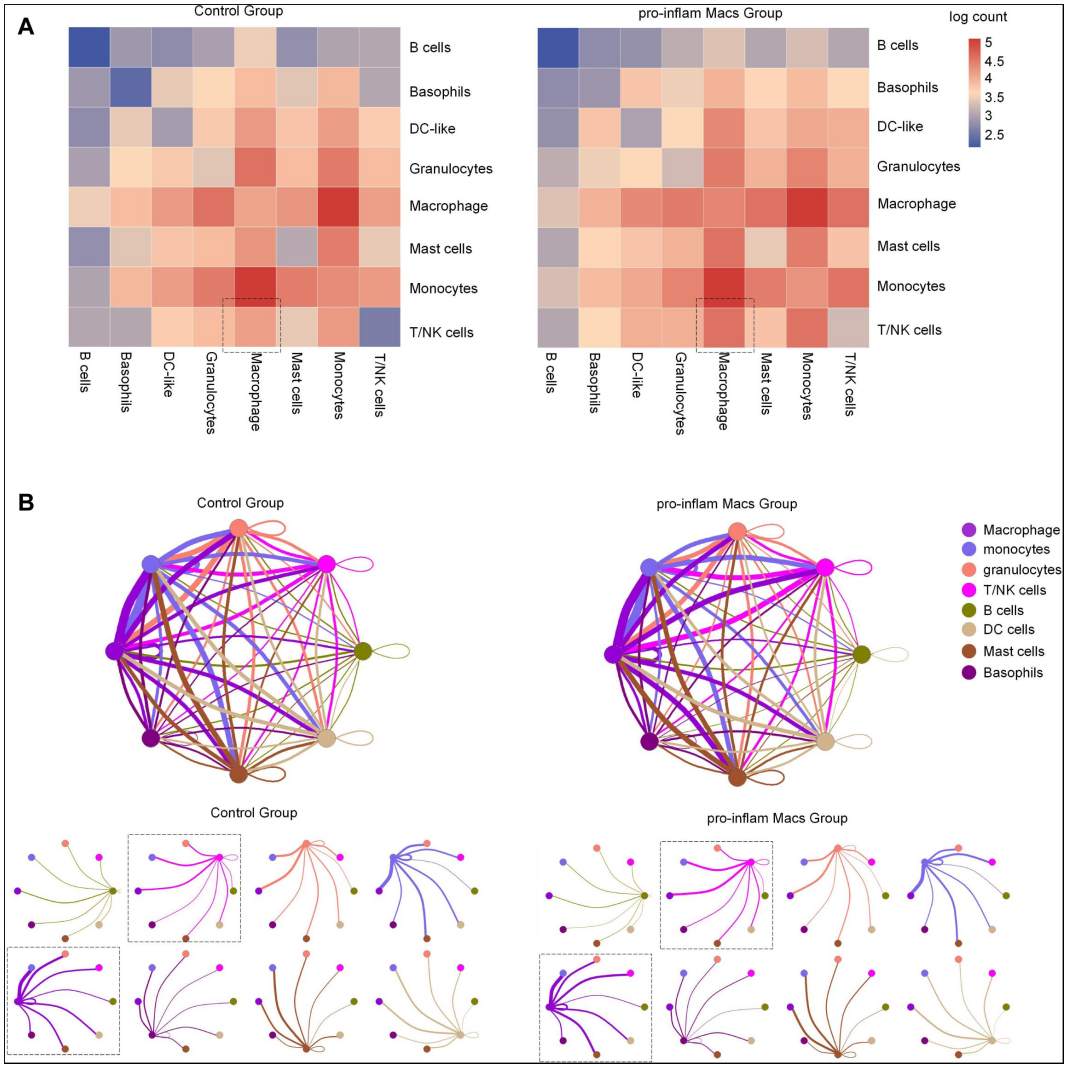

Figure 8—figure supplement 1

Cell–cell communications in immune cells when pro-inflam Macs accumulated at the maternal–fetal interface.

(A) Abundance of connections between different cell types at the maternal-fetal interface analyzed by CellPhoneDB. (B) Capacities for interactions between immune cells are showed. Each line indicates the ligands expressed by the cell population represented by the same color (labeled). The lines connect to cell types that express cognate receptors. Line thickness is proportional to the number of ligands when cognate receptors are present in the recipient cell type.

References

Agbaglo E., Agbadi P., Tetteh J. K., Ameyaw E. K., Adu C., Nutor J. J (2022) **Trends in total fertility rate in Ghana by different inequality dimensions from 1993 to 2014** *BMC Womens Health* **22** https://doi.org/10.1186/s12905-022-01629-w

Amador C. A. *et al.* (2014) **Spironolactone decreases DOCA-salt-induced organ damage by blocking the activation of T helper 17 and the downregulation of regulatory T lymphocytes** *Hypertension* **63**:797–803 https://doi.org/10.1161/hypertensionaha.113.02883

Aneman I., Pienaar D., Suvakov S., Simic T. P., Garovic V. D., McClements L (2020) **Mechanisms of Key Innate Immune Cells in Early- and Late-Onset Preeclampsia** *Front Immunol* **11** https://doi.org/10.3389/fimmu.2020.01864

Bachmayer N., Rafik Hamad R., Liszka L., Bremme K., Sverremark-Ekström E (2006) **Aberrant uterine natural killer (NK)-cell expression and altered placental and serum levels of the NK-cell promoting cytokine interleukin-12 in pre-eclampsia** *Am J Reprod Immunol* **56**:292–301 https://doi.org/10.1111/j.1600-0897.2006.00429.x

Bekkering S. *et al.* (2018) **Metabolic Induction of Trained Immunity through the Mevalonate Pathway** *Cell* **172**:135–146 https://doi.org/10.1016/j.cell.2017.11.025

Bernardes T. P., Mol B. W., Ravelli A. C. J., van den Berg P. P., Boezen H. M., Groen H. (2019) **Recurrence risk of preeclampsia in a linked population-based cohort: Effects of first pregnancy maximum diastolic blood pressure and gestational age** *Pregnancy Hypertens* **15**:32–36 https://doi.org/10.1016/j.preghy.2018.10.010

Burton G. J., Redman C. W., Roberts J. M., Moffett A (2019) **Pre-eclampsia: pathophysiology and clinical implications** *Bmj* **366** https://doi.org/10.1136/bmj.l2381

Care A. S., Bourque S. L., Morton J. S., Hjartarson E. P., Robertson S. A., Davidge S. T (2018) **Reduction in Regulatory T Cells in Early Pregnancy Causes Uterine Artery Dysfunction in Mice** *Hypertension* **72**:177–187 https://doi.org/10.1161/hypertensionaha.118.10858

Chappell L. C., Cluver C. A., Kingdom J., Tong S (2021) **Pre-eclampsia** *Lancet* **398**:341–354 https://doi.org/10.1016/s0140-6736(20)32335-7

Chatterjee P. *et al.* (2017) **Depletion of MHC class II invariant chain peptide or γ-δ T-cells ameliorates experimental preeclampsia** *Clin Sci (Lond* **131**:2047–2058 https://doi.org/10.1042/cs20171008

Chen B., Ye B., Li M., Wang S., Li J., Lai Y., Yang N., Ke Z., Zhang H (2022) **TIGIT Deficiency Protects Mice From DSS-Induced Colitis by Regulating IL-17A-Producing CD4(+) Tissue-Resident Memory T Cells** *Front Immunol* **13** https://doi.org/10.3389/fimmu.2022.931761

Cornelius D. C. *et al.* (2015) **An increased population of regulatory T cells improves the pathophysiology of placental ischemia in a rat model of preeclampsia** *Am J Physiol Regul Integr Comp Physiol* **309**:R884–891 https://doi.org/10.1152/ajpregu.00154.2015

Cornelius D. C. *et al.* (2015) **Blockade of CD40 ligand for intercellular communication reduces hypertension, placental oxidative stress, and AT1-AA in response to adoptive transfer of CD4+ T lymphocytes from RUPP rats** *Am J Physiol Regul Integr Comp Physiol* **309**:R1243–1250 https://doi.org/10.1152/ajpregu.00273.2015

Corrêa-Silva S., Alencar A. P., Moreli J. B., Borbely A. U., de S. L. L., Scavone C., Damasceno D. C., Rudge M. V. C., Bevilacqua E., Calderon I. M. P. (2018) **Hyperglycemia induces inflammatory mediators in the human chorionic villous** *Cytokine* **111**:41–48 https://doi.org/10.1016/j.cyto.2018.07.020

Deer E., Herrock O., Campbell N., Cornelius D., Fitzgerald S., Amaral L. M., LaMarca B (2023) **The role of immune cells and mediators in preeclampsia** *Nat Rev Nephrol* **19**:257–270 https://doi.org/10.1038/s41581-022-00670-0

Deer E. *et al.* (2021) **CD4+ T cells cause renal and placental mitochondrial oxidative stress as mechanisms of hypertension in response to placental ischemia** *Am J Physiol Renal Physiol* **320**:F47–f54 https://doi.org/10.1152/ajprenal.00398.2020

Díaz E., Cárdenas M., Ariza A. C., Larrea F., Halhali A (2005) **Placental insulin and insulin-like growth factor I receptors in normal and preeclamptic pregnancies** *Clin Biochem* **38**:243–247 https://doi.org/10.1016/j.clinbiochem.2004.10.013

DiToro D. *et al.* (2020) **Insulin-Like Growth Factors Are Key Regulators of T Helper 17 Regulatory T Cell Balance in Autoimmunity** *Immunity* **52**:650–667 https://doi.org/10.1016/j.immuni.2020.03.013

Eghbal-Fard S. *et al.* (2019) **The imbalance of Th17/Treg axis involved in the pathogenesis of preeclampsia** *J Cell Physiol* **234**:5106–5116 https://doi.org/10.1002/jcp.27315

Faas M. M., Spaans F., De Vos P. (2014) **Monocytes and macrophages in pregnancy and pre-eclampsia** *Front Immunol* **5** https://doi.org/10.3389/fimmu.2014.00298

Fanelli G. *et al.* (2021) **PD-L1 signaling on human memory CD4+ T cells induces a regulatory phenotype** *PLoS Biol* **19** https://doi.org/10.1371/journal.pbio.3001199

Fu B., Li X., Sun R., Tong X., Ling B., Tian Z., Wei H (2013) **Natural killer cells promote immune tolerance by regulating inflammatory TH17 cells at the human maternal-fetal interface** *Proc Natl Acad Sci U S A* **110**:E231–240 https://doi.org/10.1073/pnas.1206322110

Fu B., Tian Z., Wei H (2014) **TH17 cells in human recurrent pregnancy loss and pre-eclampsia** *Cell Mol Immunol* **11**:564–570 https://doi.org/10.1038/cmi.2014.54

Fukui A., Funamizu A., Yokota M., Yamada K., Nakamua R., Fukuhara R., Kimura H., Mizunuma H (2011) **Uterine and circulating natural killer cells and their roles in women with recurrent pregnancy loss, implantation failure and preeclampsia** *J Reprod Immunol* **90**:105–110 https://doi.org/10.1016/j.jri.2011.04.006

Grotegut C. A (2016) **Prevention of preeclampsia** *J Clin Invest* **126**:4396–4398 https://doi.org/10.1172/jci91300

Han X., Li W., Li P., Zheng Z., Lin B., Zhou B., Guo K., He P., Yang J (2021) **Stimulation of α7 Nicotinic Acetylcholine Receptor by Nicotine Suppresses Decidual M1 Macrophage Polarization Against Inflammation in Lipopolysaccharide-Induced Preeclampsia-Like Mouse Model** *Front Immunol* **12** https://doi.org/10.3389/fimmu.2021.642071

Jensen F., Wallukat G., Herse F., Budner O., El-Mousleh T., Costa S. D., Dechend R., Zenclussen A. C (2012) **CD19+CD5+ cells as indicators of preeclampsia** *Hypertension* **59**:861–868 https://doi.org/10.1161/hypertensionaha.111.188276

Jiang L. *et al.* (2021) **Extracellular Vesicle-Mediated Secretion of HLA-E by Trophoblasts Maintains Pregnancy by Regulating the Metabolism of Decidual NK Cells** *Int J Biol Sci* **17**:4377–4395 https://doi.org/10.7150/ijbs.63390

Jung E., Romero R., Yeo L., Gomez-Lopez N., Chaemsaithong P., Jaovisidha A., Gotsch F., Erez O (2022) **The etiology of preeclampsia** *Am J Obstet Gynecol* **226**:S844–s866 https://doi.org/10.1016/j.ajog.2021.11.1356

Kieffer T. E. C., Laskewitz A., Scherjon S. A., Faas M. M., Prins J. R (2019) **Memory T Cells in Pregnancy** *Front Immunol* **10** https://doi.org/10.3389/fimmu.2019.00625

Köstlin-Gille N., Dietz S., Schwarz J., Spring B., Pauluschke-Fröhlich J., Poets C. F., Gille C (2019) **HIF-1α-Deficiency in Myeloid Cells Leads to a Disturbed Accumulation of Myeloid Derived Suppressor Cells (MDSC) During Pregnancy and to an Increased Abortion Rate in Mice** *Front Immunol* **10** https://doi.org/10.3389/fimmu.2019.00161

Lager S. *et al.* (2020) **Abnormal placental CD8(+) T-cell infiltration is a feature of fetal growth restriction and pre-eclampsia** *J Physiol* **598**:5555–5571 https://doi.org/10.1113/jp279532

LaMarca B., Wallace K., Herse F., Wallukat G., Martin J. N., Weimer A., Dechend R (2011) **Hypertension in response to placental ischemia during pregnancy: role of B lymphocytes** *Hypertension* **57**:865–871 https://doi.org/10.1161/hypertensionaha.110.167569

Lampé R., Kövér Á., Szűcs S., Pál L., Árnyas E., Ádány R., Póka R (2015) **Phagocytic index of neutrophil granulocytes and monocytes in healthy and preeclamptic pregnancy** *J Reprod Immunol* **107**:26–30 https://doi.org/10.1016/j.jri.2014.11.001

Lampé R., Szucs S., Adány R., Póka R (2011) **Granulocyte superoxide anion production and regulation by plasma factors in normal and preeclamptic pregnancy** *J Reprod Immunol* **89**:199–206 https://doi.org/10.1016/j.jri.2011.01.019

Lang X., Liu W., Hou Y., Zhao W., Yang X., Chen L., Yan Q., Cheng W (2021) **IL-17A polymorphism (rs2275913) and levels are associated with preeclampsia pathogenesis in Chinese patients** *BMC Med Genomics* **14** https://doi.org/10.1186/s12920-020-00840-8

Lewis E. L., Sierra L. J., Barila G. O., Brown A. G., Porrett P. M., Elovitz M. A (2018) **Placental immune state shifts with gestational age** *Am J Reprod Immunol* **79** https://doi.org/10.1111/aji.12848

Li M., Sun F., Xu Y., Chen L., Chen C., Cui L., Qian J., Li D., Wang S., Du M (2022) **Tim-3(+) decidual Mφs induced Th2 and Treg bias in decidual CD4(+)T cells and promoted pregnancy maintenance via CD132** *Cell Death Dis* **13** https://doi.org/10.1038/s41419-022-04899-2

Liao G., Cheng D., Li J., Hu S (2021) **Clinical significance of microRNA-320a and insulin-like growth factor-1 receptor in early-onset preeclampsia patients** *Eur J Obstet Gynecol Reprod Biol* **263**:164–170 https://doi.org/10.1016/j.ejogrb.2021.06.032

Lisonkova S., Joseph K. S (2013) **Incidence of preeclampsia: risk factors and outcomes associated with early-versus late-onset disease** *Am J Obstet Gynecol* **209**:e541–544 https://doi.org/10.1016/j.ajog.2013.08.019

Liu D. *et al.* (2021) **Placenta-derived IL-32β activates neutrophils to promote preeclampsia development** *Cell Mol Immunol* **18**:979–991 https://doi.org/10.1038/s41423-021-00636-5

Liu X. *et al.* (2022) **Trophoblast-Derived Extracellular Vesicles Promote Preeclampsia by Regulating Macrophage Polarization** *Hypertension* **79**:2274–2287 https://doi.org/10.1161/hypertensionaha.122.19244

Lu D., Peng Q., Chen D., Chen X., Jiang M (2020) **Expression imbalance of IL-17/IL-35 in peripheral blood and placental tissue of pregnant women in preeclampsia** *Taiwan J Obstet Gynecol* **59**:409–414 https://doi.org/10.1016/j.tjog.2020.03.013

Madhur M. S. *et al.* (2021) **Hypertension: Do Inflammation and Immunity Hold the Key to Solving this Epidemic?** *Circ Res* **128**:908–933 https://doi.org/10.1161/circresaha.121.318052

McElwain C. J., McCarthy F. P., McCarthy C. M (2021) **Gestational Diabetes Mellitus and Maternal Immune Dysregulation: What We Know So Far** *Int J Mol Sci* **22** https://doi.org/10.3390/ijms22084261

McIntyre H. D., Catalano P., Zhang C., Desoye G., Mathiesen E. R., Damm P (2019) **Gestational diabetes mellitus** *Nat Rev Dis Primers* **5** https://doi.org/10.1038/s41572-019-0098-8

Miller D., Garcia-Flores V., Romero R., Galaz J., Pique-Regi R., Gomez-Lopez N (2022) **Single-Cell Immunobiology of the Maternal-Fetal Interface** *J Immunol* **209**:1450–1464 https://doi.org/10.4049/jimmunol.2200433

Morita K., Tsuda S., Kobayashi E., Hamana H., Tsuda K., Shima T., Nakashima A., Ushijima A., Kishi H., Saito S (2020) **Analysis of TCR Repertoire and PD-1 Expression in Decidual and Peripheral CD8(+) T Cells Reveals Distinct Immune Mechanisms in Miscarriage and Preeclampsia** *Front Immunol* **11** https://doi.org/10.3389/fimmu.2020.01082

Nerenberg K. A., Johnson J. A., Leung B., Savu A., Ryan E. A., Chik C. L., Kaul P (2013) **Risks of gestational diabetes and preeclampsia over the last decade in a cohort of Alberta women** *J Obstet Gynaecol Can* **35**:986–994 https://doi.org/10.1016/s1701-2163(15)30786-6

Novotny S. R. *et al.* (2012) **Activating autoantibodies to the angiotensin II type I receptor play an important role in mediating hypertension in response to adoptive transfer of CD4+ T lymphocytes from placental ischemic rats** *Am J Physiol Regul Integr Comp Physiol* **302**:R1197–1201 https://doi.org/10.1152/ajpregu.00623.2011

Ostlund I., Haglund B., Hanson U (2004) **Gestational diabetes and preeclampsia** *Eur J Obstet Gynecol Reprod Biol* **113**:12–16 https://doi.org/10.1016/j.ejogrb.2003.07.001

Rasmussen T. A. *et al.* (2022) **Memory CD4(+) T cells that co-express PD1 and CTLA4 have reduced response to activating stimuli facilitating HIV latency** *Cell Rep Med* **3** https://doi.org/10.1016/j.xcrm.2022.100766

Robajac D., Masnikosa R., Miković Ž, Mandić V., Nedić O. (2015) **Oxidation of placental insulin and insulin-like growth factor receptors in mothers with diabetes mellitus or preeclampsia complicated with intrauterine growth restriction** *Free Radic Res* **49**:984–989 https://doi.org/10.3109/10715762.2015.1020798

Rowe J. H., Ertelt J. M., Xin L., Way S. S (2012) **Pregnancy imprints regulatory memory that sustains anergy to fetal antigen** *Nature* **490**:102–106 https://doi.org/10.1038/nature11462

Saito S., Shiozaki A., Nakashima A., Sakai M., Sasaki Y (2007) **The role of the immune system in preeclampsia** *Mol Aspects Med* **28**:192–209 https://doi.org/10.1016/j.mam.2007.02.006

Santner-Nanan B., Peek M. J., Khanam R., Richarts L., Zhu E., Fazekas de St Groth B., Nanan R. (2009) **Systemic increase in the ratio between Foxp3+ and IL-17-producing CD4+ T cells in healthy pregnancy but not in preeclampsia** *J Immunol* **183**:7023–7030 https://doi.org/10.4049/jimmunol.0901154

Sasaki Y., Darmochwal-Kolarz D., Suzuki D., Sakai M., Ito M., Shima T., Shiozaki A., Rolinski J., Saito S (2007) **Proportion of peripheral blood and decidual CD4(+) CD25(bright) regulatory T cells in pre-eclampsia** *Clin Exp Immunol* **149**:139–145 https://doi.org/10.1111/j.1365-2249.2007.03397.x

Schneider S., Freerksen N., Röhrig S., Hoeft B., Maul H (2012) **Gestational diabetes and preeclampsia--similar risk factor profiles?** *Early Hum Dev* **88**:179–184 https://doi.org/10.1016/j.earlhumdev.2011.08.004

Schonkeren D., van der Hoorn M. L., Khedoe P., Swings G., van Beelen E., Claas F., van Kooten C., de Heer E., Scherjon S (2011) **Differential distribution and phenotype of decidual macrophages in preeclamptic versus control pregnancies** *Am J Pathol* **178**:709–717 https://doi.org/10.1016/j.ajpath.2010.10.011

Shields C. A., McCalmon M., Ibrahim T., White D. L., Williams J. M., LaMarca B., Cornelius D. C (2018) **Placental ischemia-stimulated T-helper 17 cells induce preeclampsia-associated cytolytic natural killer cells during pregnancy** *Am J Physiol Regul Integr Comp Physiol* **315**:R336–r343 https://doi.org/10.1152/ajpregu.00061.2018

Spradley F. T., Palei A. C., Granger J. P (2015) **Immune Mechanisms Linking Obesity and Preeclampsia** *Biomolecules* **5**:3142–3176 https://doi.org/10.3390/biom5043142

Travis O. K., White D., Baik C., Giachelli C., Thompson W., Stubbs C., Greer M., Lemon J. P., Williams J. M., Cornelius D. C (2020) **Interleukin-17 signaling mediates cytolytic natural killer cell activation in response to placental ischemia** *Am J Physiol Regul Integr Comp Physiol* **318**:R1036–r1046 https://doi.org/10.1152/ajpregu.00285.2019

Wallace K., Novotny S., Heath J., Moseley J., Martin J. N., Owens M. Y., LaMarca B (2012) **Hypertension in response to CD4(+) T cells from reduced uterine perfusion pregnant rats is associated with activation of the endothelin-1 system** *Am J Physiol Regul Integr Comp Physiol* **303**:R144–149 https://doi.org/10.1152/ajpregu.00049.2012

Wang S., Zhu X., Xu Y., Zhang D., Li Y., Tao Y., Piao H., Li D., Du M (2016) **Programmed cell death-1 (PD-1) and T-cell immunoglobulin mucin-3 (Tim-3) regulate CD4+ T cells to induce Type 2 helper T cell (Th2) bias at the maternal-fetal interface** *Hum Reprod* **31**:700–711 https://doi.org/10.1093/humrep/dew019

Weissgerber T. L., Mudd L. M (2015) **Preeclampsia and diabetes** *Curr Diab Rep* **15** https://doi.org/10.1007/s11892-015-0579-4

Yao Y., Xu X. H., Jin L (2019) **Macrophage Polarization in Physiological and Pathological Pregnancy** *Front Immunol* **10** https://doi.org/10.3389/fimmu.2019.00792

Zhong X., Gao W., Degauque N., Bai C., Lu Y., Kenny J., Oukka M., Strom T. B., Rothstein T. L (2007) **Reciprocal generation of Th1/Th17 and T(reg) cells by B1 and B2 B cells** *Eur J Immunol* **37**:2400–2404 https://doi.org/10.1002/eji.200737296

Zhou J., Nefedova Y., Lei A., Gabrilovich D (2018) **Neutrophils and PMN-MDSC: Their biological role and interaction with stromal cells** *Semin Immunol* **35**:19–28 https://doi.org/10.1016/j.smim.2017.12.004

Chen X. *et al.* (2023) **Microglia-mediated T cell infiltration drives neurodegeneration in tauopathy** *Nature* **615**:668–677 https://doi.org/10.1038/s41586-023-05788-0

Chen J. *et al.* (2022) **Tumor extracellular vesicles mediate anti-PD-L1 therapy resistance by decoying anti-PD-L1** *Cell Mol Immunol* **19**:1290–1301 https://doi.org/10.1038/s41423-022-00926-6

Nalio Ramos R *et al.* (2022) **Tissue-resident FOLR2+ macrophages associate with CD8+ T cell infiltration in human breast cancer** *Cell* **185**:1189–1207 https://doi.org/10.1016/j.cell.2022.02.021

Thomas JR *et al.* (2021) **Phenotypic and functional characterization of first-trimester human placental macrophages, Hofbauer cells** *J Exp Med* **218** https://doi.org/10.1084/jem.20200891

Che LH *et al.* (2021) **A single-cell atlas of liver metastases of colorectal cancer reveals reprogramming of the tumor microenvironment in response to preoperative chemotherapy** *Cell Discov* **7** https://doi.org/10.1038/s41421-021-00312-y

Desrumaux C *et al.* (2016) **Plasma phospholipid transfer protein (PLTP) modulates adaptive immune functions through alternation of T helper cell polarization** *Cell Mol Immunol* **13**:795–804 https://doi.org/10.1038/cmi.2015.75

He J *et al.* (2019) **Fbxw7 increases CCL2/7 in CX3CR1hi macrophages to promote intestinal inflammation** *J Clin Invest* **129**:3877–3893 https://doi.org/10.1172/JCI123374

Wu Y *et al.* (2023) **FAP expression in adipose tissue macrophages promotes obesity and metabolic inflammation** *Proc Natl Acad Sci U S A* **120** https://doi.org/10.1073/pnas.2303075120

Jin G *et al.* (2023) **5-aminolevulinate and CHIL3/CHI3L1 treatment amid ischemia aids liver metabolism and reduces ischemia-reperfusion injury** *Theranostics* **13**:4802–4820 https://doi.org/10.7150/thno.83163

Nugteren S, Samsom JN (2021) **Secretory Leukocyte Protease Inhibitor (SLPI) in mucosal tissues: Protects against inflammation, but promotes cancer** *Cytokine Growth Factor Rev* **59**:22–35 https://doi.org/10.1016/j.cytogfr.2021.01.005

Li R *et al.* (2022) **Mapping single-cell transcriptomes in the intra-tumoral and associated territories of kidney cancer** *Cancer Cell* **40**:1583–1599 https://doi.org/10.1016/j.ccell.2022.11.001

Che LH *et al.* (2021) **A single-cell atlas of liver metastases of colorectal cancer reveals reprogramming of the tumor microenvironment in response to preoperative chemotherapy** *Cell Discov* **7** https://doi.org/10.1038/s41421-021-00312-y

Coppo L, Mishra P, Siefert N, Holmgren A, Pääbo S, Zeberg H (2022) **A substitution in the glutathione reductase lowers electron leakage and inflammation in modern humans** *Sci Adv* **8** https://doi.org/10.1126/sciadv.abm1148

Hang S *et al.* (2019) **Bile acid metabolites control TH17 and Treg cell differentiation** *Nature* **576**:143–148 https://doi.org/10.1038/s41586-019-1785-z

Leite JA *et al.* (2023) **AIM2 promotes TH17 cells differentiation by regulating RORγt transcription activity** *iScience* **26** https://doi.org/10.1016/j.isci.2023.108134

Evrard M *et al.* (2023) **Single-cell protein expression profiling resolves circulating and resident memory T cell diversity across tissues and infection contexts** *Immunity* **56**:1664–1680 https://doi.org/10.1016/j.immuni.2023.06.005

Bieberich F *et al.* (2021) **A Single-Cell Atlas of Lymphocyte Adaptive Immune Repertoires and Transcriptomes Reveals Age-Related Differences in Convalescent COVID-19 Patients** *Front Immunol* **12** https://doi.org/10.3389/fimmu.2021.701085

Qiu C, Du G (2022) **Loss of LEF-1 expression as a diagnostic indicator for extranodal NK/T-cell lymphoma: An immunohistochemical study of 88 cases** *Eur J Haematol* **109**:513–518 https://doi.org/10.1111/ejh.13836

Sekine T *et al.* (2020) **TOX is expressed by exhausted and polyfunctional human effector memory CD8+ T cells** *Sci Immunol* **5** https://doi.org/10.1126/sciimmunol.aba7918

Esensten JH, Helou YA, Chopra G, Weiss A, Bluestone JA (2016) **CD28 Costimulation: From Mechanism to Therapy** *Immunity* **44**:973–88 https://doi.org/10.1016/j.immuni.2016.04.020

Pai JA *et al.* (2023) **Lineage tracing reveals clonal progenitors and long-term persistence of tumor-specific T cells during immune checkpoint blockade** *Cancer Cell* **41**:776–790 https://doi.org/10.1016/j.ccell.2023.03.009

Montaldo E *et al.* (2022) **Cellular and transcriptional dynamics of human neutrophils at steady state and upon stress** *Nat Immunol* **23**:1470–1483 https://doi.org/10.1038/s41590-022-01311-1

Wenzel P *et al.* (2015) **Heme oxygenase-1 suppresses a pro-inflammatory phenotype in monocytes and determines endothelial function and arterial hypertension in mice and humans** *Eur Heart J* **36**:3437–46 https://doi.org/10.1093/eurheartj/ehv544

Ulff-Møller CJ, Asmar F, Liu Y, Svendsen AJ, Busato F, Grønbaek K, Tost J, Jacobsen S (2018) **Twin DNA Methylation Profiling Reveals Flare-Dependent Interferon Signature and B Cell Promoter Hypermethylation in Systemic Lupus Erythematosus** *Arthritis Rheumatol* **70**:878–890 https://doi.org/10.1002/art.40422

Drummond RA *et al.* (2019) **CARD9+ microglia promote antifungal immunity via IL-1β- and CXCL1-mediated neutrophil recruitment** *Nat Immunol* **20**:559–570 https://doi.org/10.1038/s41590-019-0377-2

von Wulffen M *et al.* (2023) **S100A8/A9-alarmin promotes local myeloid-derived suppressor cell activation restricting severe autoimmune arthritis** *Cell Rep* **42** https://doi.org/10.1016/j.celrep.2023.113006

Kao KD, Grasberger H, El-Zaatari M (2023) **The Cxcr2+ subset of the S100a8+ gastric granylocytic myeloid-derived suppressor cell population (G-MDSC) regulates gastric pathology** *Front Immunol* **14** https://doi.org/10.3389/fimmu.2023.1147695

Editors

Reviewing Editor
Simon Yona
The Hebrew University of Jerusalem, Jerusalem, Israel

Senior Editor
Tadatsugu Taniguchi
University of Tokyo, Tokyo, Japan

Reviewer #1 (Public review):

Summary:

In this study, the authors utilized human placental samples together with multiple mouse models to explore the mechanisms whereby inflammatory macrophages and T cells are linked to preeclampsia (PE). The authors first undertook CyTOF of placental samples from women with normal pregnancies, PE, gestational diabetes mellitus (GDM), and GDM with superimposed PE (GDM+PE). The authors report an increase of memory-like Th17 cells, memory-like CD8+ T cells, and pro-inflammatory macrophages in PE cases, but not GDM or GDM+PE, together with diminished γδT cells, anti-inflammatory macrophages, and granulocyte myeloid-derived suppressor cells (gMDSC). The authors then undertook several experiments using scRNA-seq, bulk RNA-seq, and flow cytometry in a RUPP model to first show that the transfer of pro-inflammatory macrophages from RUPP mice into normal pregnant mice with depleted macrophages resulted in increased embryo resorption and diminished fetal weight and size. Moreover, pro-inflammatory macrophages induced memory-like Th17 cells in mice. Similarly, injection of T-cells from RUPP mice resulted in increased embryo resorption and diminished fetal weight and size. Such mice that received RUPP-derived T cells displayed similarly worsened outcomes in their second pregnancy in the absence of any additional T cell transfer. The authors identified the IGF1-IGF1R ligand-receptor pair as a factor involved in the macrophage-mediated induction of memory-like Th17 cells, as confirmed by experiments using an IGF1R inhibitor. Finally, the authors transferred IGF1R inhibitor-treated T cells to a pregnant mouse that was administered LPS and depleted of T cells and observed improved outcomes compared to mice that received non-treated T cells. The authors conclude that their study identifies a PE-specific immune cell network regulated by pro-inflammatory macrophages and T cells.

Strengths:

Utilization of both human placental samples and multiple mouse models to explore the mechanisms linking inflammatory macrophages and T cells to preeclampsia (PE). Incorporation of advanced techniques such as CyTOF, scRNA-seq, bulk RNA-seq, and flow cytometry.

Identification of specific immune cell populations and their roles in PE, including the IGF1-IGF1R ligand-receptor pair in macrophage-mediated Th17 cell differentiation.
Demonstration of the adverse effects of pro-inflammatory macrophages and T cells on pregnancy outcomes through transfer experiments.

Weaknesses:

Inconsistent use of uterine and placental cells, which are distinct tissues with different macrophage populations, potentially confounding results.

Missing observational data for the initial experiment transferring RUPP-derived macrophages to normal pregnant mice.

Unclear mechanisms of anti-macrophage compounds and their effects on placental/fetal macrophages.

Difficulty in distinguishing donor cells from recipient cells in murine single-cell data complicates interpretation.

Limitation of using the LPS model in the final experiments, as it more closely resembles systemic inflammation seen in endotoxemia rather than the specific pathology of PE.

https://doi.org/10.7554/eLife.100002.1.sa2

Reviewer #2 (Public review):

Summary:

Fei, Lu, Shi, et al. present a thorough evaluation of the immune cell landscape in pre-eclamptic human placentas by single-cell multi-omics methodologies compared to normal control placentas. Based on their findings of elevated frequencies of inflammatory macrophages and memory-like Th17 cells, they employ adoptive cell transfer mouse models to interrogate the coordination and function of these cell types in pre-eclampsia immunopathology. They demonstrate the putative role of the IGF1-IGF1R axis as the key pathway by which inflammatory macrophages in the placenta skew CD4+ T cells towards an inflammatory IL-17A-secreting phenotype that may drive tissue damage, vascular dysfunction, and elevated blood pressure in pre-eclampsia, leaving researchers with potential translational opportunities to pursue this pathway in this indication.

They present a major advance to the field in their profiling of human placental immune cells from pre-eclampsia patients where most extant single-cell atlases focus on term versus preterm placenta, or largely examine trophoblast biology with a much rarer subset of immune cells. While the authors present vast amounts of data at both the protein and RNA transcript level, we, the reviewers, feel this manuscript is still in need of much more clarity in its main messaging, and more discretion in including only key data that supports this main message most effectively.

Strengths:

(1) This study combines human and mouse analyses and allows for some amount of mechanistic insight into the role of pro-inflammatory and anti-inflammatory macrophages in the pathogenesis of pre-eclampsia (PE), and their interaction with Th17 cells.

(2) Importantly, they do this using matched cohorts across normal pregnancy and common PE comorbidities like gestation diabetes (GDM).

(3) The authors have developed clear translational opportunities from these "big data" studies by moving to pursue potential IGF1-based interventions.

Weaknesses:

(1) Clearly the authors generated vast amounts of multi-omic data using CyTOF and single-cell RNA-seq (scRNA-seq), but their central message becomes muddled very quickly. The reader has to do a lot of work to follow the authors' multiple lines of inquiry rather than smoothly following along with their unified rationale. The title description tells fairly little about the substance of the study. The manuscript is very challenging to follow. The paper would benefit from substantial reorganizations and editing for grammatical and spelling errors. For example, RUPP is introduced in Figure 4 but in the text not defined or even talked about what it is until Figure 6. (The figure comparing pro- and anti-inflammatory macrophages does not add much to the manuscript as this is an expected finding).

(2) The methods lack critical detail about how human placenta samples were processed. The maternal-fetal interface is a highly heterogeneous tissue environment and care must be taken to ensure proper focus on maternal or fetal cells of origin. Lacking this detail in the present manuscript, there are many unanswered questions about the nature of the immune cells analyzed. It is impossible to figure out which part of the placental unit is analyzed for the human or mouse data. Is this the decidua, the placental villi, or the fetal membranes? This is of key importance to the central findings of the manuscript as the immune makeup of these compartments is very different. Or is this analyzed as the entirety of the placenta, which would be a mix of these compartments and significantly less exciting?

(3) Similarly, methods lack any detail about the analysis of the CyTOF and scRNAseq data, much more detail needs to be added here. How were these clustered, what was the QC for scRNAseq data, etc? The two small paragraphs lack any detail.

(4) There is also insufficient detail presented about the quantities or proportions of various cell populations. For example, gdT cells represent very small proportions of the CyTOF plots shown in Figures 1B, 1C, & 1E, yet in Figures 2I, 2K, & 2K there are many gdT cells shown in subcluster analysis without a description of how many cells are actually represented, and where they came from. How were biological replicates normalized for fair statistical comparison between groups?

(5) The figures themselves are very tricky to follow. The clusters are numbered rather than identified by what the authors think they are, the numbers are so small, that they are challenging to read. The paper would be significantly improved if the clusters were clearly labeled and identified. All the heatmaps and the abundance of clusters should be in separate supplementary figures.

(6) The authors should take additional care when constructing figures that their biological replicates (and all replicates) are accurately represented. Figure 2H-2K shows N=10 data points for the normal pregnant (NP) samples when clearly their Table 1 and test denote they only studied N=9 normal subjects.

(7) There is little to no evaluation of regulatory T cells (Tregs) which are well known to undergird maternal tolerance of the fetus, and which are well known to have overlapping developmental trajectory with RORgt+ Th17 cells. We recommend the authors evaluate whether the loss of Treg function, quantity, or quality leaves CD4+ effector T cells more unrestrained in their effect on PE phenotypes. References should include, accordingly: PMCID: PMC6448013 / DOI: 10.3389/fimmu.2019.00478; PMC4700932 / DOI: 10.1126/science.aaa9420.

(8) In discussing gMDSCs in Figure 3, the authors have missed key opportunities to evaluate bona fide Neutrophils. We recommend they conduct FACS or CyTOF staining including CD66b if they have additional tissues or cells available. Please refer to this helpful review article that highlights key points of distinguishing human MDSC from neutrophils: https://doi.org/10.1038/s41577-024-01062-0. This will both help the evaluation of potentially regulatory myeloid cells that may suppress effector T cells as well as aid in understanding at the end of the study if IL-17 produced by CD4+ Th17 cells might recruit neutrophils to the placenta and cause ROS immunopathology and fetal resorption.

(9) Depletion of macrophages using several different methodologies (PLX3397, or clodronate liposomes) should be accompanied by supplementary data showing the efficiency of depletion, especially within tissue compartments of interest (uterine horns, placenta). The clodronate piece is not at all discussed in the main text. Both should be addressed in much more detail.

(10) There are many heatmaps and tSNE / UMAP plots with unhelpful labels and no statistical tests applied. Many of these plots (e.g. Figure 7) could be moved to supplemental figures or pared down and combined with existing main figures to help the authors streamline and unify their message.

(11) There are claims that this study fills a gap that "only one report has provided an overall analysis of immune cells in the human placental villi in the presence and absence of spontaneous labor at term by scRNA-seq (Miller 2022)" (lines 362-364), yet this study itself does not exhaustively study all immune cell subsets...that's a monumental task, even with the two multi-omic methods used in this paper. There are several other datasets that have performed similar analyses and should be referenced.

(12) Inappropriate statistical tests are used in many of the analyses. Figures 1-2 use the Shapiro-Wilk test, which is a test of "goodness of fit", to compare unpaired groups. A Kruskal-Wallis or other nonparametric t-test is much more appropriate. In other instances, there is no mention of statistical tests (Figures 6-7) at all. Appropriate tests should be added throughout.

https://doi.org/10.7554/eLife.100002.1.sa1

Author response:

> ***Reviewer #1:***
>
> *Strengths:*
>
> *Utilization of both human placental samples and multiple mouse models to explore the mechanisms linking inflammatory macrophages and T cells to preeclampsia (PE). Incorporation of advanced techniques such as CyTOF, scRNA-seq, bulk RNA-seq, and flow cytometry.*
>
> *Identification of specific immune cell populations and their roles in PE, including the IGF1-IGF1R ligand-receptor pair in macrophage-mediated Th17 cell differentiation. Demonstration of the adverse effects of pro-inflammatory macrophages and T cells on pregnancy outcomes through transfer experiments.*
>
> *Weaknesses:*
>
> *Comment 1. Inconsistent use of uterine and placental cells, which are distinct tissues with different macrophage populations, potentially confounding results.*

Response1: We thank the reviewers' comments. We have done the green fluorescent protein (GFP) pregnant mice-related animal experiment, which was not shown in this manuscript. The wild-type (WT) female mice were mated with either transgenic male mice, genetically modified to express GFP, or with WT male mice, in order to generate either GFP-expressing pups (GFP-pups) or their genetically unmodified counterparts (WT-pups), respectively. Mice were euthanized on day 18.5 of gestation, and the uteri of the pregnant females and the placentas of the offspring were analyzed using flow cytometry. The majority of macrophages in the uterus and placenta are of maternal origin, which was defined by GFP negative. In contrast, fetal-derived macrophages, distinguished by their expression of GFP, represent a mere fraction of the total macrophage population, signifying their inconsequential or restricted presence amidst the broader cellular landscape. We will added the GPF pregnant mice-related data in Figure 4-figure supplement 1 to explain the different macrophage populations in the uterine and placental cells.

> *Comment 2. Missing observational data for the initial experiment transferring RUPP-derived macrophages to normal pregnant mice.*

Response 2: We thank the reviewers' comments. In our experiments, PLX3397 or Clodronate Liposomes was used to deplete the macrophages of pregnant mice, and then we injected RUPP-derived pro-inflammatory macrophages and anti-inflammatory macrophages back into PLX3397 or Clodronate Liposomes-treated pregnant mice. And We found that RUPP-derived F480+CD206- pro-inflammatory macrophages induced immune imbalance at the maternal-fetal interface and PE-like symptoms (Figure 4E-4H and Figure 4-figure supplement 1 A-C).

> *Comment 3. Unclear mechanisms of anti-macrophage compounds and their effects on placental/fetal macrophages.*

Response 3: We thank the reviewers' comments. PLX3397, the inhibitor of CSF1R, which is needed for macrophage development (Nature. 2023, PMID: 36890231; Cell Mol Immunol. 2022, PMID: 36220994), we have stated that on line 189-191. However, PLX3397 is a small molecule compound that possesses the potential to cross the placental barrier and affect fetal macrophages. We will discuss the impact of this factor on the experiment in the discussion section.

> *Comment 4. Difficulty in distinguishing donor cells from recipient cells in murine single-cell data complicates interpretation.*

Response 4: We thank the reviewers' comments. Upon analysis, we observed a notable elevation in the frequency of total macrophages within the CD45+ cell population. Then we subsequently performed macrophage clustering and uncovered a marked increase in the frequency of Cluster 0, implying a potential correlation between Cluster 0 and donor-derived cells. RNA sequencing revealed that the F480+CD206- pro-inflammatory donor macrophages exhibited a Folr2+Ccl7+Ccl8+C1qa+C1qb+C1qc+ phenotype, which is consistent with the phenotype of cluster 0 in macrophages observed in single-cell RNA sequencing (Figure 4D and Figure 5E). Therefore, we believe that the donor cells is cluster 0 in macrophages.

> *Comment 5. Limitation of using the LPS model in the final experiments, as it more closely resembles systemic inflammation seen in endotoxemia rather than the specific pathology of PE.*

Response 5: We thank the reviewers' comments. Firstly, our other animal experiments in this manuscript used the Reduction in Uterine Perfusion Pressure (RUPP) mouse model to simulate the pathology of PE. However, the RUPP model requires ligation of the uterine

arteries in pregnant mice on day 12.5 of gestation, which hinders T cells returning from the tail vein from reaching the maternal-fetal interface. In addition, this experiment aims to prove that CD4+ T cells are differentiated into memory-like Th17 cells through IGF-1R receptor signalling to affect pregnancy by clearing CD4+ T cells in vivo with an anti-CD4 antibody followed by injecting IGF-1R inhibitor-treated CD4+ T cells. And we proved that injection of RUPP-derived memory-like CD4+ T cells into pregnant rats induces PE-like symptoms (Figure 6). In summary, the application of the LPS model in Figure 8 does not affect the conclusions.

> ***Reviewer #2:***
>
> *Strengths:*
>
> *(1) This study combines human and mouse analyses and allows for some amount of mechanistic insight into the role of pro-inflammatory and anti-inflammatory macrophages in the pathogenesis of pre-eclampsia (PE), and their interaction with Th17 cells.*
>
> *(2) Importantly, they do this using matched cohorts across normal pregnancy and common PE comorbidities like gestation diabetes (GDM).*
>
> *(3) The authors have developed clear translational opportunities from these "big data" studies by moving to pursue potential IGF1-based interventions.*
>
> *Weaknesses:*
>
> *Comment 1. Clearly the authors generated vast amounts of multi-omic data using CyTOF and single-cell RNA-seq (scRNA-seq), but their central message becomes muddled very quickly. The reader has to do a lot of work to follow the authors' multiple lines of inquiry rather than smoothly following along with their unified rationale. The title description tells fairly little about the substance of the study. The manuscript is very challenging to follow. The paper would benefit from substantial reorganizations and editing for grammatical and spelling errors. For example, RUPP is introduced in Figure 4 but in the text not defined or even talked about what it is until Figure 6. (The figure comparing pro- and anti-inflammatory macrophages does not add much to the manuscript as this is an expected finding).*

Response 1: We thank the reviewers' comments. According to the reviewer's suggestion, we will proceed with making the necessary revisions. Firstly, We will modify the title of the article to be more specific. Then, we will introduce the RUPP mouse model when interpreted Figure 4. Thirdly, we plan to simplify or consolidate the images from Figure5 to Figure7 to make them easier to follow. Finally, We will diligently correct the grammatical and spelling errors in the article. As for the figure comparing pro- and anti-inflammatory macrophages, The Editor requested a more comprehensive description of the macrophage phenotype during the initial submission. As a result, we conducted the transcriptomes of both uterine-derived pro-inflammatory and anti-inflammatory macrophages and conducted a detailed analysis of macrophages in single-cell data.

> *Comment 2. The methods lack critical detail about how human placenta samples were processed. The maternal-fetal interface is a highly heterogeneous tissue environment and care must be taken to ensure proper focus on maternal or fetal cells of origin. Lacking this detail in the present manuscript, there are many unanswered questions about the nature of the immune cells analyzed. It is impossible to figure out which part of the placental unit is analyzed for the human or mouse data. Is this the decidua, the placental villi, or the fetal membranes? This is of key importance to the central findings of the manuscript as the immune makeup of these compartments is very different. Or is this*

> *analyzed as the entirety of the placenta, which would be a mix of these compartments and significantly less exciting?*

Response 2: We thank the reviewers' comments. Placental villi rather than fetal membranes and decidua were used for CyToF in this study. This detail about how human placenta samples were processed will be added to the Materials and Methods section.

> *Comment 3. Similarly, methods lack any detail about the analysis of the CyTOF and scRNAseq data, much more detail needs to be added here. How were these clustered, what was the QC for scRNAseq data, etc? The two small paragraphs lack any detail.*

Response 3: We thank the reviewers' comments. The detail about the analysis of the CyTOF and scRNAseq data will be added in the Materials and Methods section.

> *Comment 4. There is also insufficient detail presented about the quantities or proportions of various cell populations. For example, gdT cells represent very small proportions of the CyTOF plots shown in Figures 1B, 1C, & 1E, yet in Figures 2I, 2K, & 2K there are many gdT cells shown in subcluster analysis without a description of how many cells are actually represented, and where they came from. How were biological replicates normalized for fair statistical comparison between groups?*

Response 4: We thank the reviewers' comments. In Figure 1, CD45+ immune cells were clustered into 10 subpopulations, which included gdT cells. While Figure 2 displays the further clustering analysis of CD4+T, CD8+T, and gdT cells, with gdT cells being further subdivided into 22 clusters (Figure 2-figure supplement 1C). The number of biological replicates (samples) is consistent with Figure 1.

> *Comment 5. The figures themselves are very tricky to follow. The clusters are numbered rather than identified by what the authors think they are, the numbers are so small, that they are challenging to read. The paper would be significantly improved if the clusters were clearly labeled and identified. All the heatmaps and the abundance of clusters should be in separate supplementary figures.*

Response 5: We thank the reviewers' comments. The t-SNE distributions of the 15 clusters of CD4+ T cells, 18 clusters of CD8+ T cells, and 22 clusters of gdT cells are shown separately in Figure 2A, F, and I. The heatmaps displaying the expression levels of markers in these clusters of CD4+ T cells, CD8+ T cells, and gdT cells are presented in Figure 2-figure supplement 1A, B, and C, respectively. The t-SNE distributions of the 29 clusters of CD11b+ cells are shown in Figure 3A, and the heatmap displaying the expression levels of markers in these clusters is presented in Figure 3B. As for sc-RNA sequencing, the heatmap and UMAP distributions of the 15 clusters of macrophages are shown separately in Figure 5C and 5D. The UMAP distributions and heatmap of the 12 clusters of T/NK cells are shown in Figure 6A and 6B. The UMAP distributions and heatmap of the 9 clusters of T/NK cells are shown in Figure 7A and 7B.

> *Comment 6. The authors should take additional care when constructing figures that their biological replicates (and all replicates) are accurately represented. Figure 2H-2K shows N=10 data points for the normal pregnant (NP) samples when clearly their Table 1 and test denote they only studied N=9 normal subjects.*

Response 6: We thank the reviewers' careful checking. During our verification, we found that one sample in the NP group had pregnancy complications other than PE and GMD. The data in Figure 2H-2K was not updated in a timely manner. We will promptly update this data and reanalyze it.

> *Comment 7. There is little to no evaluation of regulatory T cells (Tregs) which are well known to undergird maternal tolerance of the fetus, and which are well known to have overlapping developmental trajectory with RORgt+ Th17 cells. We recommend the authors evaluate whether the loss of Treg function, quantity, or quality leaves CD4+ effector T cells more unrestrained in their effect on PE phenotypes. References should include, accordingly: PMCID: PMC6448013 / DOI: 10.3389/fimmu.2019.00478; PMC4700932 / DOI: 10.1126/science.aaa9420.*

Response 7: We thank the reviewers' comments. We have done the Treg-related animal experiment, which was not shown in this manuscript. We will add the Treg-related data in Figure 6. The injection of CD4+ T cells derived from RUPP mouse, characterized by a reduced frequency of Tregs, could induce PE-like symptoms in pregnant mice. Additionally, we will add a necessary discussion about Tregs.

> *Comment 8. In discussing gMDSCs in Figure 3, the authors have missed key opportunities to evaluate bona fide Neutrophils. We recommend they conduct FACS or CyTOF staining including CD66b if they have additional tissues or cells available. Please refer to this helpful review article that highlights key points of distinguishing human MDSC from neutrophils: https://doi.org/10.1038/s41577-024-01062-0. This will both help the evaluation of potentially regulatory myeloid cells that may suppress effector T cells as well as aid in understanding at the end of the study if IL-17 produced by CD4+ Th17 cells might recruit neutrophils to the placenta and cause ROS immunopathology and fetal resorption.*

Response 8: We thank the reviewers' comments. Although we do not have additional tissues or cells available to conduct FACS or CyTOF staining, including for CD66b, we plan to utilize CD15 and CD66b antibodies for immunofluorescence staining of placental tissue. Suppressing effector T cells is a signature feature of MDSCs, and T cells may also influence the functions of MDSCs, we will refer to this review and discuss it in the Discussion section of the article.

> *Comment 9. Depletion of macrophages using several different methodologies (PLX3397, or clodronate liposomes) should be accompanied by supplementary data showing the efficiency of depletion, especially within tissue compartments of interest (uterine horns, placenta). The clodronate piece is not at all discussed in the main text. Both should be addressed in much more detail.*

Response 9: We thank the reviewers' comments. We already have the additional data on the efficiency ofmacrophage depletion involving PLX3397 and clodronate liposomes, which were not present in this manuscript, and we'll add it to the manuscript. The clodronate piece is mentioned in the main text (Line 197-201), but only briefly described, because the results using clodronate we obtained were similar to those using PLX3397.

> *Comment 10. There are many heatmaps and tSNE / UMAP plots with unhelpful labels and no statistical tests applied. Many of these plots (e.g. Figure 7) could be moved to supplemental figures or pared down and combined with existing main figures to help the authors streamline and unify their message.*

Response 10: We thank the reviewers' comments. We plan to simplify or consolidate the images from Figure5 to Figure7 to make them easier to follow.

> *Comment 11. There are claims that this study fills a gap that "only one report has provided an overall analysis of immune cells in the human placental villi in the presence and absence of spontaneous labor at term by scRNA-seq (Miller 2022)" (lines 362-364),*

> *yet this study itself does not exhaustively study all immune cell subsets...that's a monumental task, even with the two multi-omic methods used in this paper. There are several other datasets that have performed similar analyses and should be referenced.*

Response 11: We thank the reviewers' comments. We will search for more literature and reference additional studies that have conducted similar analyses.

> *Comment 12. Inappropriate statistical tests are used in many of the analyses. Figures 1-2 use the Shapiro-Wilk test, which is a test of "goodness of fit", to compare unpaired groups. A Kruskal-Wallis or other nonparametric t-test is much more appropriate. In other instances, there is no mention of statistical tests (Figures 6-7) at all. Appropriate tests should be added throughout.*

We thank the reviewers' comments. As stated in the Statistical Analysis section (lines 601-604), the Kruskal-Wallis test was used to compare the results of experiments with multiple groups. Comparisons between the two groups in Figures 6-7 were conducted using Student's t-test. The aforementioned statistical methods will be included in the figure legends.

https://doi.org/10.7554/eLife.100002.1.sa0